

How to fix a broken confidence estimator: Evaluating post-hoc methods for selective classification with deep neural networks

Luís Felipe P. Cattelan, Danilo Silva

Department of Electrical and Electronic Engineering

Federal University of Santa Catarina (UFSC)

Florianópolis, Brazil

lfp.cattelan@gmail.com, danilo.silva@ufsc.br

October 5, 2023

Abstract

This paper addresses the problem of selective classification for deep neural networks, where a model is allowed to abstain from low-confidence predictions to avoid potential errors. We focus on so-called post-hoc methods, which replace the confidence estimator of a given classifier without retraining or modifying it, thus being practically appealing. Considering neural networks with softmax outputs, our goal is to identify the best confidence estimator that can be computed directly from the unnormalized logits. This problem is motivated by the intriguing observation in recent work that many classifiers appear to have a “broken” confidence estimator, in the sense that their selective classification performance is much worse than what could be expected by their corresponding accuracies. We perform an extensive experimental study of many existing and proposed confidence estimators applied to 84 pretrained ImageNet classifiers available from popular repositories. Our results show that a simple p -norm normalization of the logits, followed by taking the maximum logit as the confidence estimator, can lead to considerable gains in selective classification performance, completely fixing the pathological behavior observed in many classifiers. As a consequence, the selective classification performance of any classifier becomes almost entirely determined by its corresponding accuracy. Moreover, these results are shown to be consistent under distribution shift. We also investigate why certain classifiers innately have a good confidence estimator that apparently cannot be improved by post-hoc methods.

1 Introduction

Consider a machine learning classifier that does not reach the desired performance for the intended application, even after significant development time. This may occur for a variety of reasons: the problem is too hard for the current technology; more development resources (data, compute or time) are needed than what is economically feasible for the specific situation; or perhaps the target distribution is different from the training one. In this case, then, should the model *not* be deployed?

Selective classification Geifman & El-Yaniv (2017); El-Yaniv & Wiener (2010) offers a potential solution, which can be seen as a last resort. The idea is to reject predictions for which the model is least confident, hoping to increase the performance on the accepted predictions. The rejected inputs may be processed in the same way as if the model were not deployed, for instance, by a human specialist or by the previously existing system. This imposes a burden on the deployed model, which is run for all inputs but is useful only for a subset of them. Still, it offers a tradeoff between performance and *coverage* (the proportion of accepted predictions) which may be a better solution than any of the extremes. In particular, it could shorten the path to adoption of deep learning especially in critical applications, such as medical diagnosis and autonomous driving, where the consequences of erroneous decisions can be severe (Zou et al., 2023; Neumann et al., 2018).

A key element in selective classification is the confidence estimator that is thresholded to decide whether a prediction is accepted. In the case of neural networks with softmax outputs, the natural baseline to be used as a confidence

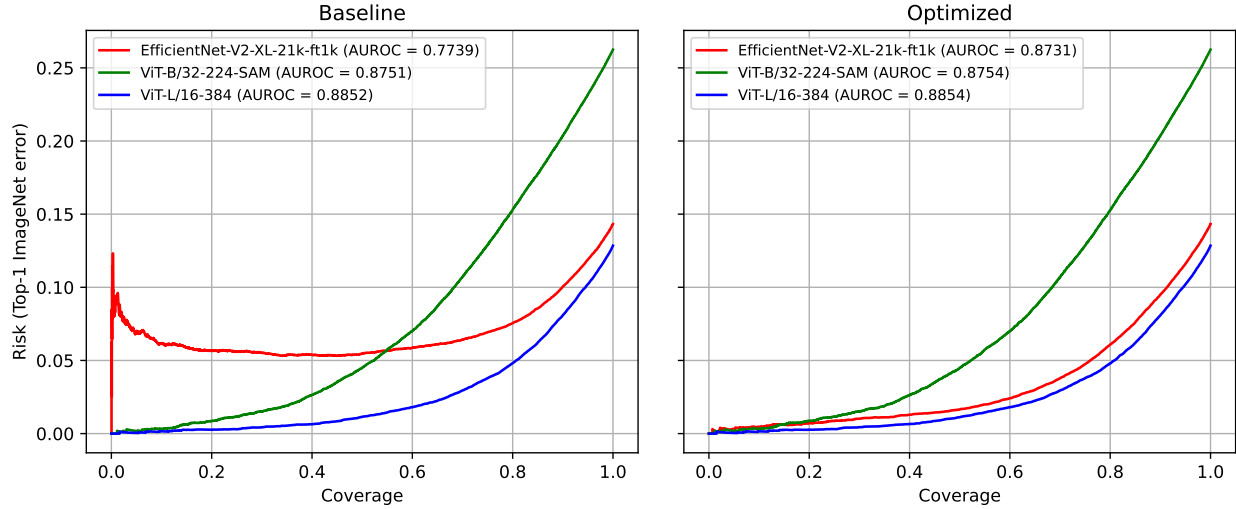


Figure 1: A comparison of RC curves made by three models selected in (Galil et al., 2023), including examples of highest (ViT-L/16-384) and lowest (EfficientNet-V2-XL) AUROC. After the application of a simple post-hoc method, the apparent pathology in EfficientNet-V2-XL completely disappears, resulting in significantly improved selective classification performance.

estimator is the maximum softmax probability (MSP) produced by the model, also known as the softmax response (Geifman & El-Yaniv, 2017; Hendrycks & Gimpel, 2016). Several approaches have been proposed attempting to improve upon this baseline, which generally fall into two categories: approaches that require retraining the classifier, by modifying some aspect of the architecture or the training procedure, possibly adding an auxiliary head as the confidence estimator (Geifman & El-Yaniv, 2019; Liu et al., 2019a; Huang et al., 2020); and post-hoc approaches that do not require retraining, thus only modifying or replacing the confidence estimator based on outputs or intermediate features produced by the model (Corbière et al., 2022; Granese et al., 2021; Shen et al., 2022; Galil et al., 2023).¹

Post-hoc approaches not only are practically appealing, especially for large deep learning models, but also should serve as a baseline against which to compare any training-based approaches. However, a thorough evaluation of potential post-hoc estimators has not yet appeared in the literature. The work furthest in that direction is the paper by Galil et al. (2023), who empirically evaluated ImageNet classifiers and found that temperature scaling (TS) (Guo et al., 2017), a well-known post-hoc calibration method, could sometimes improve selective classification performance.

In this paper, we focus on the simplest possible class of post-hoc methods, which are those for which the confidence estimator can be computed directly from the network unnormalized *logits* (pre-softmax output). Our main goal is to identify the methods that produce the largest gains in selective classification performance, measured by the area under the risk-coverage curve (AUROC); however, as in general these methods can have hyperparameters that need to be tuned on hold-out data, we are also concerned with data efficiency. Our study is motivated by an intriguing problem reported in (Galil et al., 2023) and illustrated in Fig. 1: some state-of-the-art ImageNet classifiers, despite attaining excellent predictive performance, nevertheless exhibit appallingly poor performance at detecting their own mistakes. Can such pathologies be fixed by simple post-hoc methods?

To answer this question, we consider every such method to our knowledge, as well as several variations and novel methods that we propose, and perform an extensive experimental study using 84 pretrained ImageNet classifiers available from popular repositories. Our results show that, among other close contenders, a simple p -norm normalization of the logits, followed by taking the maximum logit as the confidence estimator, can lead to considerable gains in selective classification performance, completely fixing the pathological behavior observed in many classifiers, as illustrated in Fig. 1. As a consequence, the selective classification performance of any classifier becomes almost entirely determined by its corresponding accuracy.

¹For more complete account of related work, please see Appendix A.

In summary, the contributions of this work are:

- We propose a simple but powerful framework for designing confidence estimators, which involves tunable logit transformations optimized directly for a selective classification metric;
- We perform an extensive experimental study of many existing and proposed confidence estimators applied to 84 pretrained ImageNet classifiers available from popular repositories. In particular, we show that simple post-hoc estimators, such as the max-logit normalized by the logit p -norm, can provide up to 62% reduction in normalized AURC using no more than one sample per class of labeled hold-out data;
- We study how these post-hoc methods perform under distribution shift and find that the results remain consistent: a method that provides gains in the in-distribution scenario also provides considerable gains under distribution shift;
- We investigate why certain classifiers innately have a good confidence estimator that apparently cannot be improved by post-hoc methods.

2 Problem Formulation and Background

2.1 Selective classification

Let P be an unknown distribution over $\mathcal{X} \times \mathcal{Y}$, where \mathcal{X} is the input space and $\mathcal{Y} = \{1, \dots, C\}$ is the label space, and C is the number of classes. A *classifier* is a prediction function $h : \mathcal{X} \rightarrow \mathcal{Y}$. The classifier's (true) *risk* is $R(h) = E_P[\ell(h(x), y)]$, where $\ell : \mathcal{Y} \times \mathcal{Y} \rightarrow \mathbb{R}^+$ is a given loss function, for instance, the 0/1 loss $\ell(\hat{y}, y) = \mathbb{1}[\hat{y} \neq y]$, where $\mathbb{1}[\cdot]$ denotes the indicator function.

A *selective classifier* (Geifman & El-Yaniv, 2017) is a pair (h, g) , where h is a classifier and $g : \mathcal{X} \rightarrow \mathbb{R}$ is a *confidence estimator* (also known as *confidence score function* or *confidence-rate function*), which quantifies the model's confidence on its prediction for a given input. For some fixed threshold t , given an input x , the selective model makes a prediction $h(x)$ if $g(x) \geq t$, otherwise it abstains from making a prediction. We say that x is *selected* in the former case and *rejected* in the latter. A selective model's *coverage* $\phi(h, g) = P[g(x) \geq t]$ is the probability mass of the selected samples in \mathcal{X} , while its *selective risk* $R(h, g) = E_P[\ell(h(x), y) \mid g(x) \geq t]$ is its risk restricted to the selected samples. In particular, a model's risk equals its selective risk at *full coverage* (i.e., for t such that $\phi(h, g) = 1$). These quantities can be evaluated empirically given a given a test dataset $\{(x_i, y_i)\}_{i=1}^N$ drawn i.i.d. from P , yielding the *empirical coverage* $\hat{\phi}(h, g) = (1/N) \sum_{i=1}^N \mathbb{1}[g(x_i) \geq t]$ and the *empirical selective risk*

$$\hat{R}(h, g) = \frac{\sum_{i=1}^N \ell(h(x_i), y_i) \mathbb{1}[g(x_i) \geq t]}{\sum_{i=1}^N \mathbb{1}[g(x_i) \geq t]}. \quad (1)$$

Note that, by varying t , it is generally possible to trade off coverage for selective risk, i.e., a lower selective risk can usually (but not necessarily always) be achieved if more samples are rejected. This tradeoff is captured by the *risk-coverage (RC) curve* (Geifman & El-Yaniv, 2017), a plot of $\hat{R}(h, g)$ as a function of $\hat{\phi}(h, g)$.

While the RC curve provides a full picture of the performance of a selective classifier, it is convenient to have a scalar metric that summarizes this curve. A commonly used metric is the *area under the RC curve* (AURC) (Ding et al., 2020; Geifman et al., 2019), denoted by $\text{AURC}(h, g)$. However, when comparing selective models, if two RC curves cross, then each model may have a better selective performance than the other depending on the operating point chosen, which cannot be captured by the AURC. Another interesting metric, which forces the choice of an operating point, is the *selective accuracy constraint* (SAC) (Galil et al., 2023), defined as the minimum coverage required for a model to achieve a specified accuracy.

Misclassification detection (Hendrycks & Gimpel, 2016), which refers to the problem of discriminating between correct and incorrect predictions made by a classifier, is closely related to selective classification. Both tasks rely on ranking predictions according to their confidence estimates, where correct predictions should be ideally separated from incorrect ones. More precisely, if $(x_1, y_1), (x_2, y_2) \in \mathcal{X} \times \mathcal{Y}$ are such that $\ell(h(x_1), y_1) > \ell(h(x_2), y_2)$, then we would like to have $g(x_1) < g(x_2)$, i.e., an optimal g orders samples in decreasing order of their losses. In the case of the 0/1

loss, a natural metric of ranking performance (Galil et al., 2023) is the area under the ROC curve (AUROC) (Fawcett, 2006) for misclassification detection. This metric is blind to the classifier performance and focuses exclusively on the quality of the confidence estimates, i.e., for a given classifier h , different confidence estimators g can be compared in their ranking performance. Thus, misclassification detection can also be seen as a proxy problem on which to evaluate confidence estimators for selective classification.

2.2 Confidence estimation

From now on we restrict attention to classifiers that can be decomposed as $h(x) = \arg \max_{k \in \mathcal{Y}} z_k$, where $\mathbf{z} = f(x)$ and $f : \mathcal{X} \rightarrow \mathbb{R}^C$ is a neural network. The network output \mathbf{z} is referred to as the (vector of) *logits* or *logit vector*, due to the fact that it is typically applied to a softmax function to obtain an estimate of the posterior distribution $P[y|x]$. The softmax function is defined as

$$\sigma : \mathbb{R}^C \rightarrow [0, 1]^C, \quad \sigma_k(\mathbf{z}) = \frac{e^{z_k}}{\sum_{j=1}^C e^{z_j}}, \quad k \in \{1, \dots, C\} \quad (2)$$

where $\sigma_k(\mathbf{z})$ denotes the k th element of the vector $\sigma(\mathbf{z})$.

The most popular confidence estimator is arguably the *maximum softmax probability* (MSP) (Ding et al., 2020), also known as *maximum class probability* (Corbière et al., 2022) or *softmax response* (Geifman & El-Yaniv, 2017)

$$g(x) = \text{MSP}(\mathbf{z}) \triangleq \max_{k \in \mathcal{Y}} \sigma_k(\mathbf{z}) = \sigma_{\hat{y}}(\mathbf{z}) \quad (3)$$

where $\hat{y} = \arg \max_{k \in \mathcal{Y}} z_k$. However, other functions of the logits can be considered. Some examples are the *softmax margin* (Belghazi & Lopez-Paz, 2021; Lubrano et al., 2023), the *max logit* (Hendrycks et al., 2022), the *logits margin* (Streeter, 2018; Lebovitz et al., 2023), the *negative entropy*² (Belghazi & Lopez-Paz, 2021), and the *negative Gini index* (Granese et al., 2021; Gomes et al., 2022), defined, respectively, as

$$\text{SoftmaxMargin}(\mathbf{z}) \triangleq \sigma_{\hat{y}}(\mathbf{z}) - \max_{k \in \mathcal{Y}: k \neq \hat{y}} \sigma_k(\mathbf{z}) \quad (4)$$

$$\text{MaxLogit}(\mathbf{z}) \triangleq z_{\hat{y}} \quad (5)$$

$$\text{LogitsMargin}(\mathbf{z}) \triangleq z_{\hat{y}} - \max_{k \in \mathcal{Y}: k \neq \hat{y}} z_k \quad (6)$$

$$\text{NegativeEntropy}(\mathbf{z}) \triangleq \sum_{k \in \mathcal{Y}} \sigma_k(\mathbf{z}) \log \sigma_k(\mathbf{z}) \quad (7)$$

$$\text{NegativeGini}(\mathbf{z}) \triangleq -1 + \sum_{k \in \mathcal{Y}} \sigma_k(\mathbf{z})^2. \quad (8)$$

Note that, in the scenario we consider, DOCTOR’s D_α and D_β discriminators (Granese et al., 2021) are equivalent to the negative Gini index and MSP confidence estimators, respectively, as discussed in more detail in Appendix B.

3 Methods

3.1 Tunable Logit Transformations

In this section, we introduce a simple but powerful framework for designing post-hoc confidence estimators for selective classification. The idea is to take any parameter-free logit-based confidence estimator, such as those described in section 2.2, and augment it with a logit transformation parameterized by one or a few hyperparameters, which are then tuned (e.g., via grid search) using a labeled hold-out dataset not used during training of the classifier (i.e., validation data). Moreover, this hyperparameter tuning is done using as objective function not a proxy loss but rather the exact same metric that one is interested in optimizing, for instance, AURC or AUROC. This approach forces us to be conservative about the hyperparameter search space, which is important for data efficiency.

²Note that any uncertainty estimator can be used as a confidence estimator by taking its negative.

3.1.1 Temperature Scaling

Originally proposed in the context of post-hoc calibration, temperature scaling (TS) (Guo et al., 2017) consists in transforming the logits as $\mathbf{z}' = \mathbf{z}/T$, before applying the softmax function. The parameter $T > 0$, which is called the temperature, is then optimized over hold-out data.

The conventional way of applying TS, as proposed in (Guo et al., 2017) for calibration and referred to here as TS-NLL, consists in optimizing T with respect to the negative log-likelihood (NLL) (Murphy, 2022). Here we instead optimize T using AURC and the resulting method is referred to as TS-AURC.

Note that TS does not affect the ranking of predictions for MaxLogit and LogitsMargin, so it is not applied in this cases.

3.1.2 Logits Normalization

Inspired by Wei et al. (2022), who show that logits norms are directly related to overconfidence and propose logit normalization during training, we propose logit normalization as a post-hoc method. Additionally, we extend the normalization from the 2-norm to a general p -norm, where p is a tunable hyperparameter. Note that the argument in (Wei et al., 2022) holds unchanged for any p , as nothing in their analysis requires $p = 2$.

Thus, logit p -normalization is defined as the operation

$$\mathbf{z}' = \frac{\mathbf{z}}{\tau \|\mathbf{z}\|_p} \quad (9)$$

where $\|\mathbf{z}\|_p \triangleq (|z_1|^p + \dots + |z_C|^p)^{1/p}$, $p \in \mathbb{R}$, is the p -norm of \mathbf{z} and $\tau > 0$ is a temperature scaling parameter. Note that this transformation is a form of adaptive TS (Balanya et al., 2023), with an input-dependent temperature $\tau \|\mathbf{z}\|_p$.

Logit p -normalization introduces two hyperparameters, p and τ , which should be jointly optimized; in this case, we first optimize τ for each value of p considered and then pick the best value of p . Such a transformation, together with the optimization of p and τ , is referred to here as pNorm. The optimizing metric is always AURC and therefore it is omitted from the nomenclature of the method.

Note that, when the underlying confidence estimator is MaxLogit or LogitsMargin, the parameter τ is irrelevant and is ignored.

3.2 Evaluation Metrics

3.2.1 Normalized AURC

A common criticism of the AURC metric is that it does not allow for meaningful comparisons across problems (Geifman et al., 2019). An AURC of some arbitrary value, for instance, 0.05, may correspond to an ideal confidence estimator for one classifier (of much higher risk) and to a completely random confidence estimator for another classifier (of risk equal to 0.05). The excess AURC (E-AURC) was proposed by Geifman et al. (2019) to alleviate this problem: for a given classifier h and confidence estimator g , it is defined as $E\text{-AURC}(h, g) = \text{AURC}(h, g) - \text{AURC}(h, g^*)$, where g^* corresponds to a hypothetically optimal confidence estimator that perfectly orders samples in decreasing order of their losses. Thus, an ideal confidence estimator always has zero E-AURC.

Unfortunately, E-AURC is still highly sensitive to the classifier's risk, as shown by Galil et al. (2023), who suggested the use of AUROC instead. However, using AUROC for comparing confidence estimators has an intrinsic disadvantage: if we are using AUROC to evaluate the performance of a tunable confidence estimator, it makes sense to optimize it using this same metric. However, as AUROC and AURC are not necessarily monotonically aligned Ding et al. (2020), the resulting confidence estimator will be optimized for a different problem than the one in which we were originally interested (which is selective classification). Ideally, we would like to evaluate confidence estimators using a metric that is a monotonic function of AURC.

We propose a simple modification to E-AURC that eliminates the shortcomings pointed out in (Galil et al., 2023): normalizing by the E-AURC of a random confidence estimator, whose AURC is equal to the classifier's risk. More precisely, we define the normalized AURC (NAURC) as

$$\text{NAURC}(h, g) = \frac{\text{AURC}(h, g) - \text{AURC}(h, g^*)}{R(h) - \text{AURC}(h, g^*)}. \quad (10)$$

Note that this corresponds to a min-max scaling that maps the AURC of the ideal classifier to 0 and the AURC of the random classifier to 1. The resulting NAURC is suitable for comparison across different classifiers and is monotonically related to AURC.

3.2.2 MSP Fallback

A useful property of MSP-TS (but not MSP-TS-NLL) is that it can never have a worse performance than the MSP baseline, as long as $T = 1$ is included in the search space. It is natural to extend this property to every confidence estimator, for a simple reason: it is very easy to check whether the estimator provides an improvement to the MSP baseline and, if not, then use the MSP instead. Formally, this corresponds to adding a binary hyperparameter indicating an MSP fallback.

Equivalently, when measuring performance across different models, we simply report a (non-negligible) positive gain in NAURC whenever it occurs. More precisely, we define the *average positive gain* (APG) in NAURC as

$$\text{APG}(g) = \frac{1}{|\mathcal{H}|} \sum_{h \in \mathcal{H}} [\text{NAURC}(h, \text{MSP}) - \text{NAURC}(h, g)]_{\epsilon}^{+}, \quad [x]_{\epsilon}^{+} = \begin{cases} x, & \text{if } x > \epsilon \\ 0, & \text{otherwise} \end{cases}$$

where \mathcal{H} is a set of classifiers and $\epsilon > 0$ is chosen so that only non-negligible gains are reported.

4 Experiments

All the experiments in this section were performed using PyTorch (Paszke et al., 2019) and all of its provided classifiers pre-trained on ImageNet (Deng et al., 2009). Additionally, some models of the Wightman (2019) repository were utilized, particularly the ones highlighted by Galil et al. (2023). The list of the models, together with all the results per model are presented in Appendix H. In total, 84 ImageNet models were used for experiments. The validation set of ImageNet was randomly split into 5000 hold-out images for post-hoc optimization and 45000 for tests and comparisons. Investigations on the stability of this split are presented in Section E.

To give evidence that our results are not specific to ImageNet, we also run experiments on CIFAR-100 (Krizhevsky, 2009) and Oxford-IIIT Pet (Parkhi et al., 2012) datasets, which are presented in Appendix D.

4.1 Comparison of methods

We start by evaluating the NAURC of each possible combination of a confidence estimator listed in Section 2.2 with a logit transformation described in Section 3.1, for specific models. Table 1 and Table 2 shows the results for EfficientNet-V2-XL (trained on ImageNet-21K and fine tuned on ImageNet-1K) and VGG16, respectively, the former chosen for having the worst confidence estimator (in terms of AUROC) reported in Galil et al. (2023) and the latter chosen as a representative example of a lower accuracy model with a good confidence estimator.

Table 1: NAURC for post-hoc methods applied to an EfficientNet-V2-XL on ImageNet

Confidence Estimator	Logit Transformation			
	Raw	TS-NLL	TS-AURC	pNorm
MSP	0.4413	0.3513	0.2016	0.1722
SoftmaxMargin	0.3816	0.3143	0.2033	0.1719
MaxLogit	0.7695	–	–	0.1696
LogitsMargin	0.1935	–	–	0.1731
NegativeEntropy	0.5964	0.4286	0.2012	0.1712
NegativeGini	0.4485	0.3514	0.2067	0.1717

Table 2: NAURC for post-hoc methods applied to VGG16 on ImageNet

Confidence Estimator	Logit Transformation			
	Raw	TS-NLL	TS-AURC	pNorm
MSP	0.1838	0.1850	0.1836	0.1836
SoftmaxMargin	0.1898	0.1889	0.1887	0.1887
MaxLogit	0.3375	–	–	0.2022
LogitsMargin	0.2047	–	–	0.2047
NegativeEntropy	0.1968	0.2055	0.1837	0.1837
NegativeGini	0.1856	0.1888	0.1837	0.1837

As can be seen, on EfficientNet-V2-XL, the baseline MSP is easily outperformed by most methods. Surprisingly, the best method is not to use a softmax function but, instead, take the maximum of a p -normalized logit vector, leading to a reduction in NAURC of 0.27 points or about 62%.

However, on VGG16, the situation is quite different, as methods that use the unnormalized logits and improve the performance on EfficientNet-V2-XL, such as LogitsMargin and MaxLogit-pNorm, actually degrade it on VGG16. Moreover, the highest improvement obtained, e.g., with MSP-TS-AURC, is so small that it can be considered negligible. (In fact, gains below 0.003 NAURC are visually imperceptible in an AURC curve.) Thus, it is reasonable to assert that none of the post-hoc methods considered is able to outperform the baseline in this case.

Note that the baseline VGG16 and the optimized EfficientNet-V2-XL have NAURC values on a similar range, so we can interpret that VGG16 has innately already a good confidence estimator.

In Table 3, we evaluate the average performance of post-hoc methods across all models considered, using the APG-NAURC metric described in Section 3.2.2, where we assume $\epsilon = 0.01$. Figure 2 shows the gains for selected methods for each model, ordered by MaxLogit-pNorm gains. It can be seen that the highest gains are provided by MaxLogit-pNorm, MSP-pNorm, NegativeGini-pNorm and their performance is essentially indistinguishable whenever they provide a non-negligible gain over the baseline. Moreover, the set of models for which significant gains can be obtained appears to be consistent across all methods.

Table 3: APG-NAURC of post-hoc methods across 84 ImageNet classifiers

Confidence Estimator	Logit Transformation			
	Raw	TS-NLL	TS-AURC	pNorm
MSP	0.0	0.03622	0.05506	0.06704
SoftmaxMargin	0.01950	0.04058	0.05363	0.06513
MaxLogit	0.0	–	–	0.06752
LogitsMargin	0.05419	–	–	0.06080
NegativeEntropy	0.0	0.01565	0.05668	0.06684
NegativeGini	0.0	0.03593	0.05552	0.06701

Although several post-hoc methods provide considerable gains, they all share a practical limitation which is the requirement of hold-out data for hyperparameter tuning. (A notable exception is LogitsMargin, which provides significant gains without having any hyperparameter.) In Appendix E, we study the data efficiency of some of the best performing methods. MaxLogit-pNorm, having a single hyperparameter, emerges as a clear winner, requiring fewer than 500 samples to achieve near-optimal performance on ImageNet (< 0.5 images per class on average) and fewer than 100 samples on CIFAR-100 (< 1 image per class on average). These requirements are clearly easily satisfied in practice for typical validation set sizes.

Details on the optimization of T and p , additional results showing AUROC values and RC curves, and results on the insensitivity of our conclusions to the choice of ϵ are provided in Appendix C.

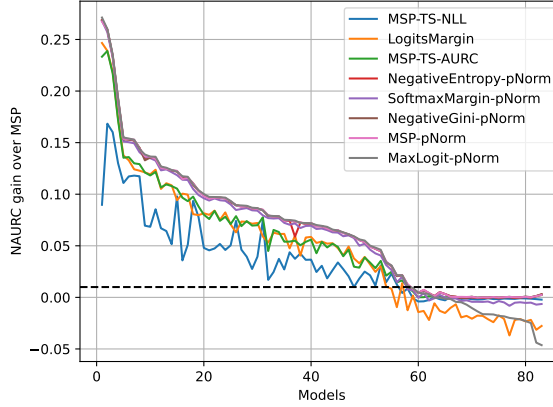


Figure 2: NAURC gains for post-hoc methods across 84 ImageNet classifiers. The dashed line denotes $\epsilon = 0.01$.

4.2 Post-hoc optimization fixes broken confidence estimators

From Figure 2, we can distinguish two groups of models: those for which the MSP baseline is already the best confidence estimator and those for which post-hoc methods provide considerable gains (particularly, MaxLogit-pNorm). In fact, most models belong to the second group, comprising 58 out of 84 models considered.

Figure 3 illustrates two noteworthy phenomena. First, as previously observed by Galil et al. (2023), certain models exhibit superior accuracy than others but poorer uncertainty estimation, leading to a trade-off when selecting a classifier for selective classification. Second, post-hoc optimization can fix any “broken” confidence estimators. This can be seen in two ways: in Figure 3a, after optimization, all models exhibit roughly the same level of confidence estimation performance (as measured by NAURC), although we can still see some dependency on accuracy (better predictive models are slightly better at predicting their own failures). In Figure 3b, it is clear that, after optimization, the selective classification performance of any classifier (as measured by AURC) becomes almost entirely determined by its corresponding accuracy. Indeed, the Spearman correlation between AURC and accuracy becomes extremely close to 1. This implies that any “broken” confidence estimators have been fixed and, consequently, total accuracy becomes the primary determinant of selective performance even at lower coverage levels.

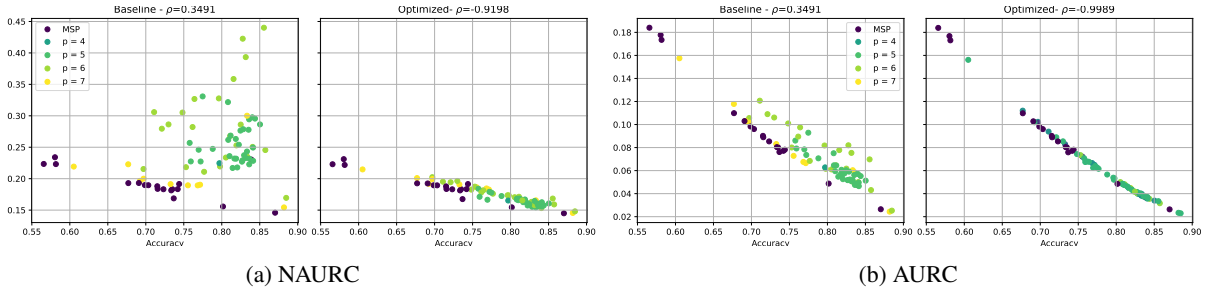


Figure 3: NAURC and AURC of 84 ImageNet classifiers with respect to their accuracy, before and after post-hoc optimization with MaxLogit-pNorm. ρ is the Spearman correlation between the metric and the corresponding accuracy. The legend shows the optimal value of p for each model, where MSP indicates MSP fallback (no significant positive gain).

An intriguing question is what properties of a classifier make it bad at confidence estimation. Experiments investigating this question were conducted and presented in Appendix F. In summary, our surprising conclusion is that models that produce highly confident MSPs tend to have better confidence estimators (in terms of NAURC), while

models whose MSP distribution is more balanced tend to be easily improvable by post-hoc optimization—which, in turn, makes the resulting confidence estimator concentrated on highly confident values.

4.3 Performance under distribution shift

We now turn to the question of how post-hoc methods for selective classification perform under distribution shift. Previous works have shown that calibration can be harmed under distribution shift, especially when certain post-hoc methods—such as temperature scaling—are applied (Ovadia et al., 2019). To investigate whether a similar issue occurs for selective classification, we evaluate selected post-hoc methods on ImageNet-C (Hendrycks & Dietterich, 2018), which consists in 15 different corruptions of the ImageNet’s validation set, and on ImageNetV2 (Recht et al., 2019), which is an independent sampling of the ImageNet test set replicating the original dataset creation process. We follow the standard approach for evaluating robustness with these datasets, which is to use them only for inference; thus, the post-hoc methods are optimized using only the 5000 hold-out images from the uncorrupted ImageNet validation dataset.

Table 4 shows the SAC metric for a ResNet50 under distribution shift, with the target accuracy as the original accuracy obtained with the “in distribution” data. As can be seen, MaxLogit-pNorm achieves higher coverages for all distribution shifts considered, significantly improving coverage over the MSP baseline. This robustness can be explained by a strong correlation between the selective performance in the original test set and under distribution shift, as discussed in Appendix G. These results provide evidence that optimizing confidence estimators on the original dataset also improves selective classification performance on the shifted dataset.

Table 4: Selective classification performance for a ResNet-50 on ImageNet under distribution shift. The target accuracy is the one achieved for corruption level 0 (i.e., 80.86%).

		Corruption level							
		Method	0	1	2	3	4	5	V2
Accuracy [%]	-		80.86	68.56	60.03	51.85	39.44	27.09	69.97
Coverage (SAC) [%]	MSP		100	75.97	56.79	41.43	21.65	9.09	76.66
	MSP-TS-AURC		100	77.13	60.51	45.49	27.41	13.32	77.29
	MaxLogit-pNorm		100	78.52	62.39	47.76	29.67	15.66	79.00

5 Conclusion

In this paper, we addressed the problem of selective multiclass classification for deep neural networks with softmax outputs. Specifically, we considered the design of post-hoc confidence estimators that can be computed directly from the unnormalized logits and proposed a simple but powerful framework that involves applying tunable logit transformations optimized directly for a selective classification metric. In order to enable meaningful comparisons of confidence estimators across classifiers of different accuracies, we proposed a normalized version of the AURC metric that is insensitive to the classifier accuracy. We then performed extensive experiments comparing 20 confidence estimators across 84 ImageNet classifiers and observed that, for 58 of these models, considerable NAURC gains can be obtained. In particular, the MaxLogit-pNorm method emerges as a clear winner, providing the highest gains with exceptional data efficiency, requiring on average less than 1 sample per class of hold-out data for tuning its single hyperparameter. These observations are also confirmed under additional datasets and shown to be consistent even under distribution shift.

We further observe that, after post-hoc optimization, all models achieve approximately the same level of confidence estimation performance, even models that have been previously shown to be very poor at this task. In particular, the selective classification performance of any classifier becomes almost entirely determined by its corresponding accuracy, eliminating the seemingly existing tradeoff between these two goals reported in previous work.

It is worth emphasizing that post-hoc optimization does not always provide significant gains: some classifiers innately have a good confidence estimator that apparently cannot be improved by post-hoc methods (and we give clues

on how to spot these classifiers just by looking at a histogram of their confidence values). However, post-hoc methods are extremely simple to apply on top of any trained classifier and should be considered the baseline against which to compare any approach that requires retraining. In fact, we advocate that post-hoc optimization be used by default when evaluating the selective classification performance of any model or training-based method, analogously to the argument made by Wang et al. (2021) and Ashukha et al. (2020) in the context of calibration.

References

Moloud Abdar, Farhad Pourpanah, Sadiq Hussain, Dana Rezazadegan, Li Liu, Mohammad Ghavamzadeh, Paul Fieguth, Xiaochun Cao, Abbas Khosravi, U. Rajendra Acharya, Vladimir Makarenkov, and Saeid Nahavandi. A Review of Uncertainty Quantification in Deep Learning: Techniques, Applications and Challenges. *Information Fusion*, 76:243–297, December 2021. ISSN 15662535. doi: 10.1016/j.inffus.2021.05.008. URL <http://arxiv.org/abs/2011.06225>. arXiv:2011.06225 [cs].

Taiga Abe, Estefany Kelly Buchanan, Geoff Pleiss, Richard Zemel, and John P. Cunningham. Deep Ensembles Work, But Are They Necessary? *Advances in Neural Information Processing Systems*, 35:33646–33660, December 2022. URL https://proceedings.neurips.cc/paper_files/paper/2022/hash/da18c47118a2d09926346f33bebde9f4-Abstract-Conference.html.

Arsenii Ashukha, Dmitry Molchanov, Alexander Lyzhov, and Dmitry Vetrov. PITFALLS OF IN-DOMAIN UNCERTAINTY ESTIMATION AND ENSEMBLING IN DEEP LEARNING. 2020.

M. Ayhan and Philipp Berens. Test-time Data Augmentation for Estimation of Heteroscedastic Aleatoric Uncertainty in Deep Neural Networks. April 2018. URL <https://www.semanticscholar.org/paper/Test-time-Data-Augmentation-for-Estimation-of-in-Ayhan-Berens/172df6d55b81f184ab0042c49634ccf9b72ed253>.

Sergio A. Balanya, Daniel Ramos, and Juan Maroñas. Adaptive Temperature Scaling for Robust Calibration of Deep Neural Networks, March 2023. URL <https://papers.ssrn.com/abstract=4379258>.

Mohamed Ishmael Belghazi and David Lopez-Paz. What classifiers know what they don’t?, July 2021. URL <http://arxiv.org/abs/2107.06217>. arXiv:2107.06217 [cs].

Luís Felipe P. Cattelan and Danilo Silva. On the performance of uncertainty estimation methods for deep-learning based image classification models. In *Anais do Encontro Nacional de Inteligência Artificial e Computacional (ENIAC)*, pp. 532–543. SBC, November 2022. doi: 10.5753/niac.2022.227603. URL <https://sol.sbc.org.br/index.php/niac/article/view/22810>. ISSN: 2763-9061.

Lucas Clarté, Bruno Loureiro, Florent Krzakala, and Lenka Zdeborová. Expectation consistency for calibration of neural networks, March 2023. URL <http://arxiv.org/abs/2303.02644>. arXiv:2303.02644 [cs, stat].

Charles Corbière, Nicolas Thome, Antoine Saporta, Tuan-Hung Vu, Matthieu Cord, and Patrick Pérez. Confidence Estimation via Auxiliary Models. *IEEE Transactions on Pattern Analysis and Machine Intelligence*, 44(10):6043–6055, October 2022. ISSN 1939-3539. doi: 10.1109/TPAMI.2021.3085983. Conference Name: IEEE Transactions on Pattern Analysis and Machine Intelligence.

Jia Deng, Wei Dong, Richard Socher, Li-Jia Li, Kai Li, and Li Fei-Fei. ImageNet: A large-scale hierarchical image database. In *2009 IEEE Conference on Computer Vision and Pattern Recognition*, pp. 248–255, June 2009. doi: 10.1109/CVPR.2009.5206848. ISSN: 1063-6919.

Yukun Ding, Jinglan Liu, Jinjun Xiong, and Yiyu Shi. Revisiting the Evaluation of Uncertainty Estimation and Its Application to Explore Model Complexity-Uncertainty Trade-Off. In *2020 IEEE/CVF Conference on Computer Vision and Pattern Recognition Workshops (CVPRW)*, pp. 22–31, Seattle, WA, USA, June 2020. IEEE. ISBN 978-1-72819-360-1. doi: 10.1109/CVPRW50498.2020.00010. URL <https://ieeexplore.ieee.org/document/9150782/>.

Ran El-Yaniv and Yair Wiener. On the Foundations of Noise-free Selective Classification. *Journal of Machine Learning Research*, 11(53):1605–1641, 2010. ISSN 1533-7928. URL <http://jmlr.org/papers/v11/el-yaniv10a.html>.

Tom Fawcett. An introduction to ROC analysis. *Pattern Recognition Letters*, 27(8):861–874, June 2006. ISSN 0167-8655. doi: 10.1016/j.patrec.2005.10.010. URL <https://www.sciencedirect.com/science/article/pii/S016786550500303X>.

Leo Feng, Mohamed Osama Ahmed, Hossein Hajimirsadeghi, and Amir H. Abdi. Towards Better Selective Classification. February 2023. URL https://openreview.net/forum?id=5gDz_yTcst.

Yarin Gal and Zoubin Ghahramani. Dropout as a Bayesian Approximation: Representing Model Uncertainty in Deep Learning. In *Proceedings of The 33rd International Conference on Machine Learning*, pp. 1050–1059. PMLR, June 2016. URL <https://proceedings.mlr.press/v48/gal16.html>. ISSN: 1938-7228.

Ido Galil, Mohammed Dabbah, and Ran El-Yaniv. What Can we Learn From The Selective Prediction And Uncertainty Estimation Performance Of 523 Imagenet Classifiers? February 2023. URL [https://openreview.net/forum?id=p66AzKi6Xim&referrer=%5BAuthor%20Console%5D\(%2Fgroup%3Fid%3DICLR.cc%2F2023%2FConference%2FAuthors%23your-submissions\)](https://openreview.net/forum?id=p66AzKi6Xim&referrer=%5BAuthor%20Console%5D(%2Fgroup%3Fid%3DICLR.cc%2F2023%2FConference%2FAuthors%23your-submissions)).

Jakob Gawlikowski, Cedrique Rovile Njieutcheu Tassi, Mohsin Ali, Jongseok Lee, Matthias Humt, Jianxiang Feng, Anna Kruspe, Rudolph Triebel, Peter Jung, Ribana Roscher, Muhammad Shahzad, Wen Yang, Richard Bamler, and Xiao Xiang Zhu. A Survey of Uncertainty in Deep Neural Networks, January 2022. URL <http://arxiv.org/abs/2107.03342>. arXiv:2107.03342 [cs, stat].

Yonatan Geifman and Ran El-Yaniv. Selective Classification for Deep Neural Networks, June 2017. URL <http://arxiv.org/abs/1705.08500>. arXiv:1705.08500 [cs].

Yonatan Geifman and Ran El-Yaniv. SelectiveNet: A Deep Neural Network with an Integrated Reject Option. In *Proceedings of the 36th International Conference on Machine Learning*, pp. 2151–2159. PMLR, May 2019. URL <https://proceedings.mlr.press/v97/geifman19a.html>. ISSN: 2640-3498.

Yonatan Geifman, Guy Uziel, and Ran El-Yaniv. Bias-Reduced Uncertainty Estimation for Deep Neural Classifiers, April 2019. URL <http://arxiv.org/abs/1805.08206>. arXiv:1805.08206 [cs, stat].

Eduardo Dadalto Câmara Gomes, Marco Romanelli, Federica Granese, and Pablo Piantanida. A simple Training-Free Method for Rejection Option. September 2022. URL <https://openreview.net/forum?id=K1DdnjL6p7>.

Julius Gonsior, Christian Falkenberg, Silvio Magino, Anja Reusch, Maik Thiele, and Wolfgang Lehner. To Softmax, or not to Softmax: that is the question when applying Active Learning for Transformer Models, October 2022. URL <http://arxiv.org/abs/2210.03005>. arXiv:2210.03005 [cs].

Federica Granese, Marco Romanelli, Daniele Gorla, Catuscia Palamidessi, and Pablo Piantanida. Doctor: A simple method for detecting misclassification errors. *Advances in Neural Information Processing Systems*, 34:5669–5681, 2021.

Chuan Guo, Geoff Pleiss, Yu Sun, and Kilian Q. Weinberger. On Calibration of Modern Neural Networks. In *Proceedings of the 34th International Conference on Machine Learning*, pp. 1321–1330. PMLR, July 2017. URL <https://proceedings.mlr.press/v70/guo17a.html>. ISSN: 2640-3498.

Kilian Hendrickx, Lorenzo Perini, Dries Van der Plas, Wannes Meert, and Jesse Davis. Machine learning with a reject option: A survey. *ArXiv*, abs/2107.11277, 2021.

Dan Hendrycks and Thomas Dietterich. Benchmarking Neural Network Robustness to Common Corruptions and Perturbations. December 2018. URL <https://openreview.net/forum?id=HJz6tiCqYm>.

Dan Hendrycks and Kevin Gimpel. A baseline for detecting misclassified and out-of-distribution examples in neural networks. *arXiv preprint arXiv:1610.02136*, 2016.

Dan Hendrycks, Steven Basart, Mantas Mazeika, Andy Zou, Joseph Kwon, Mohammadreza Mostajabi, Jacob Steinhardt, and Dawn Song. Scaling Out-of-Distribution Detection for Real-World Settings. In *Proceedings of the 39th International Conference on Machine Learning*, pp. 8759–8773. PMLR, June 2022. URL <https://proceedings.mlr.press/v162/hendrycks22a.html>.

Lang Huang, Chao Zhang, and Hongyang Zhang. Self-Adaptive Training: beyond Empirical Risk Minimization. In *Advances in Neural Information Processing Systems*, volume 33, pp. 19365–19376. Curran Associates, Inc., 2020. URL <https://proceedings.neurips.cc/paper/2020/hash/e0ab531ec312161511493b002f9be2ee-Abstract.html>.

Zixuan Jiang, Jiaqi Gu, and David Z. Pan. NormSoftmax: Normalize the Input of Softmax to Accelerate and Stabilize Training. February 2023. URL <https://openreview.net/forum?id=4g7nCbpjNwd>.

Archit Karandikar, Nicholas Cain, Dustin Tran, Balaji Lakshminarayanan, Jonathon Shlens, Michael Curtis Mozer, and Rebecca Roelofs. Soft Calibration Objectives for Neural Networks. November 2021. URL <https://openreview.net/forum?id=-tVD13hOsQ3>.

Simon Kornblith, Ting Chen, Honglak Lee, and Mohammad Norouzi. Why Do Better Loss Functions Lead to Less Transferable Features? In *Advances in Neural Information Processing Systems*, volume 34, pp. 28648–28662. Curran Associates, Inc., 2021. URL https://proceedings.neurips.cc/paper_files/paper/2021/hash/f0bf4a2da952528910047c31b6c2e951-Abstract.html.

Alex Krizhevsky. Learning Multiple Layers of Features from Tiny Images. 2009.

Balaji Lakshminarayanan, Alexander Pritzel, and Charles Blundell. Simple and Scalable Predictive Uncertainty Estimation using Deep Ensembles. In *Advances in Neural Information Processing Systems*, volume 30. Curran Associates, Inc., 2017. URL <https://proceedings.neurips.cc/paper/2017/hash/9ef2ed4b7fd2c810847ffa5fa85bce38-Abstract.html>.

Y. Le Cun, O. Matan, B. Boser, J.S. Denker, D. Henderson, R.E. Howard, W. Hubbard, L.D. Jacket, and H.S. Baird. Handwritten zip code recognition with multilayer networks. In *10th International Conference on Pattern Recognition [1990] Proceedings*, volume ii, pp. 35–40 vol.2, June 1990. doi: 10.1109/ICPR.1990.119325.

Luzian Lebovitz, Lukas Cavigelli, Michele Magno, and Lorenz K. Muller. Efficient Inference With Model Cascades. *Transactions on Machine Learning Research*, May 2023. ISSN 2835-8856. URL <https://openreview.net/forum?id=obB415rg8q>.

Shiyu Liang, Yixuan Li, and R. Srikant. Enhancing The Reliability of Out-of-distribution Image Detection in Neural Networks. May 2023. URL <https://openreview.net/forum?id=H1VGkIxRZ>.

Weitang Liu, Xiaoyun Wang, John Owens, and Yixuan Li. Energy-based out-of-distribution detection. *Advances in neural information processing systems*, 33:21464–21475, 2020.

Ziyin Liu, Zhikang Wang, Paul Pu Liang, Russ R Salakhutdinov, Louis-Philippe Morency, and Masahito Ueda. Deep Gamblers: Learning to Abstain with Portfolio Theory. In *Advances in Neural Information Processing Systems*, volume 32. Curran Associates, Inc., 2019a. URL https://proceedings.neurips.cc/paper_files/paper/2019/hash/0c4b1eeb45c90b52fb9d07943d855ab-Abstract.html.

Ziyin Liu, Zhikang Wang, Paul Pu Liang, Russ R Salakhutdinov, Louis-Philippe Morency, and Masahito Ueda. Deep gamblers: Learning to abstain with portfolio theory. *Advances in Neural Information Processing Systems*, 32, 2019b.

Mélanie Lubrano, Yaëlle Bellahsen-Harrar, Rutger Fick, Cécile Badoual, and Thomas Walter. Simple and efficient confidence score for grading whole slide images. *arXiv preprint arXiv:2303.04604*, 2023.

Jooyoung Moon, Jihyo Kim, Younghak Shin, and Sangheum Hwang. Confidence-Aware Learning for Deep Neural Networks. In *Proceedings of the 37th International Conference on Machine Learning*, pp. 7034–7044. PMLR, November 2020. URL <https://proceedings.mlr.press/v119/moon20a.html>. ISSN: 2640-3498.

Jishnu Mukhoti, Viveka Kulharia, Amartya Sanyal, Stuart Golodetz, Philip Torr, and Puneet Dokania. Calibrating Deep Neural Networks using Focal Loss. In *Advances in Neural Information Processing Systems*, volume 33, pp. 15288–15299. Curran Associates, Inc., 2020. URL <https://proceedings.neurips.cc/paper/2020/hash/aeb7b30ef1d024a76f21a1d40e30c302-Abstract.html>.

Kevin P. Murphy. *Probabilistic Machine Learning: An Introduction*. MIT Press, 2022. URL probml.ai.

Lukas Neumann, Andrew Zisserman, and Andrea Vedaldi. Relaxed softmax: Efficient confidence auto-calibration for safe pedestrian detection. 2018.

Yaniv Ovadia, Emily Fertig, Jie Ren, Zachary Nado, D. Sculley, Sebastian Nowozin, Joshua Dillon, Balaji Lakshminarayanan, and Jasper Snoek. Can you trust your model’s uncertainty? Evaluating predictive uncertainty under dataset shift. In *Advances in Neural Information Processing Systems*, volume 32. Curran Associates, Inc., 2019. URL <https://papers.nips.cc/paper/2019/hash/8558cb408c1d76621371888657d2eb1d-Abstract.html>.

Omar Parkhi, Andrea Vedaldi, Andrew Zisserman, and CV Jawahar. Oxfordiiit pet dataset. [Online]. Available from: <https://www.robots.ox.ac.uk/~vgg/data/pets/>, 2012. Accessed: 2023-09-28.

Adam Paszke, Sam Gross, Francisco Massa, Adam Lerer, James Bradbury, Gregory Chanan, Trevor Killeen, Zeming Lin, Natalia Gimelshein, Luca Antiga, Alban Desmaison, Andreas Kopf, Edward Yang, Zachary DeVito, Martin Raison, Alykhan Tejani, Sasank Chilamkurthy, Benoit Steiner, Lu Fang, Junjie Bai, and Soumith Chintala. PyTorch: An Imperative Style, High-Performance Deep Learning Library. In *Advances in Neural Information Processing Systems*, volume 32. Curran Associates, Inc., 2019. URL https://papers.nips.cc/paper_files/paper/2019/hash/bdbca288fee7f92f2bfa9f7012727740-Abstract.html.

Amir Rahimi, Thomas Mensink, Kartik Gupta, Thalaiyasingam Ajanthan, Cristian Sminchisescu, and Richard Hartley. Post-hoc Calibration of Neural Networks by g-Layers, February 2022. URL <http://arxiv.org/abs/2006.12807> [cs, stat].

Benjamin Recht, Rebecca Roelofs, Ludwig Schmidt, and Vaishaal Shankar. Do imagenet classifiers generalize to imagenet? In *International conference on machine learning*, pp. 5389–5400. PMLR, 2019.

Maohao Shen, Yuheng Bu, Prasanna Sattigeri, Soumya Ghosh, Subhro Das, and Gregory Wornell. Post-hoc Uncertainty Learning using a Dirichlet Meta-Model, December 2022. URL <http://arxiv.org/abs/2212.07359>. arXiv:2212.07359 [cs].

Matthew Streeter. Approximation Algorithms for Cascading Prediction Models. In *Proceedings of the 35th International Conference on Machine Learning*, pp. 4752–4760. PMLR, July 2018. URL <https://proceedings.mlr.press/v80/streeter18a.html>.

Mattias Teye, Hossein Azizpour, and Kevin Smith. Bayesian Uncertainty Estimation for Batch Normalized Deep Networks. In *Proceedings of the 35th International Conference on Machine Learning*, pp. 4907–4916. PMLR, July 2018. URL <https://proceedings.mlr.press/v80/teye18a.html>. ISSN: 2640-3498.

Christian Tomani, Daniel Cremers, and Florian Buettner. Parameterized Temperature Scaling for Boosting the Expressive Power in Post-Hoc Uncertainty Calibration, September 2022. URL <http://arxiv.org/abs/2102.12182>. arXiv:2102.12182 [cs].

Deng-Bao Wang, Lei Feng, and Min-Ling Zhang. Rethinking Calibration of Deep Neural Networks: Do Not Be Afraid of Overconfidence. In *Advances in Neural Information Processing Systems*, volume 34, pp. 11809–11820. Curran Associates, Inc., 2021. URL <https://proceedings.neurips.cc/paper/2021/hash/61f3a6dbc9120ea78ef75544826c814e-Abstract.html>.

Hongxin Wei, Renchunzi Xie, Hao Cheng, Lei Feng, Bo An, and Yixuan Li. Mitigating Neural Network Overconfidence with Logit Normalization. In *Proceedings of the 39th International Conference on Machine Learning*, pp. 23631–23644. PMLR, June 2022. URL <https://proceedings.mlr.press/v162/wei22d.html>. ISSN: 2640-3498.

Ross Wightman. Pytorch Image Model, 2019. URL <https://github.com/huggingface/pytorch-image-models>.

Guoxuan Xia and Christos-Savvas Bouganis. On the Usefulness of Deep Ensemble Diversity for Out-of-Distribution Detection, September 2022. URL <http://arxiv.org/abs/2207.07517>. arXiv:2207.07517 [cs].

Xu-Yao Zhang, Guo-Sen Xie, Xiuli Li, Tao Mei, and Cheng-Lin Liu. A Survey on Learning to Reject. *Proceedings of the IEEE*, 111(2):185–215, February 2023. ISSN 1558-2256. doi: 10.1109/JPROC.2023.3238024. Conference Name: Proceedings of the IEEE.

Fei Zhu, Zhen Cheng, Xu-Yao Zhang, and Cheng-Lin Liu. Rethinking Confidence Calibration for Failure Prediction. In Shai Avidan, Gabriel Brostow, Moustapha Cissé, Giovanni Maria Farinella, and Tal Hassner (eds.), *Computer Vision – ECCV 2022*, volume 13685, pp. 518–536. Springer Nature Switzerland, Cham, 2022. ISBN 978-3-031-19805-2 978-3-031-19806-9. doi: 10.1007/978-3-031-19806-9_30. URL https://link.springer.com/10.1007/978-3-031-19806-9_30. Series Title: Lecture Notes in Computer Science.

Ke Zou, Zhihao Chen, Xuedong Yuan, Xiaojing Shen, Meng Wang, and Huazhu Fu. A Review of Uncertainty Estimation and its Application in Medical Imaging, February 2023. URL <http://arxiv.org/abs/2302.08119>. arXiv:2302.08119 [cs, eess].

A Related Work

Selective prediction is also known as learning with a reject option (see (Zhang et al., 2023; Hendrickx et al., 2021) and references therein), where the rejector is usually a thresholded confidence estimator. Essentially the same problem is studied under the equivalent terms misclassification detection (Hendrycks & Gimpel, 2016), failure prediction (Corbière et al., 2022; Zhu et al., 2022), and (ordinal) ranking (Moon et al., 2020; Galil et al., 2023). Uncertainty estimation is a more general term that encompasses these tasks (where confidence may be taken as negative uncertainty) as well as other tasks where uncertainty might be useful, such as calibration and out-of-distribution (OOD) detection, among others (Gawlikowski et al., 2022; Abdar et al., 2021). These tasks are generally not aligned: for instance, optimizing for calibration may harm selective classification performance (Ding et al., 2020; Zhu et al., 2022; Galil et al., 2023). Our focus here is on in-distribution selective classification, although we also study robustness to distribution shift.

Interestingly, the same principles of selective classification can be applied to enable efficient inference with model cascades (Lebovitz et al., 2023), although the literature on those topics appears disconnected.

Most approaches to selective classification consider the base model as part of the learning problem (Geifman & El-Yaniv, 2019; Huang et al., 2020; Liu et al., 2019b), which we refer to as training-based approaches. While such an approach has a theoretical appeal, the fact that it requires retraining a model is a significant practical drawback. Alternatively, one may keep the model fixed and only modify or replace the confidence estimator, which is known as a post-hoc approach. Such an approach is practically appealing and perhaps more realistic, as it does not require retraining. Papers that follow this approach typically construct a *meta-model* that feeds on intermediate features of the base model and is trained to predict whether or not the base model is correct on hold-out samples (Corbière et al., 2022; Shen et al., 2022). However, depending on the size of such a meta-model, its training may still be computationally demanding.

A popular tool in the uncertainty literature is the use of ensembles (Lakshminarayanan et al., 2017; Teye et al., 2018; Ayhan & Berens, 2018), of which Monte-Carlo dropout Gal & Ghahramani (2016) is a prominent example. While constructing a confidence estimator from ensemble component outputs may be considered post-hoc if the ensemble is already trained, the fact that multiple inference passes need to be performed significantly increases the computational burden at test time. Moreover, recent work has found evidence that ensembles may not be fundamental for uncertainty

but simply better predictive models (Abe et al., 2022; Cattelan & Silva, 2022; Xia & Bouganis, 2022). Thus, we do not consider ensembles here.

In this work we focus on simple post-hoc confidence estimators for softmax networks that can be directly computed from the logits. The earliest example of such a post-hoc method used for selective classification in a real-world application seems to be the use of LogitsMargin in (Le Cun et al., 1990). While potentially suboptimal, such methods are extremely simple to apply on top of any trained classifier and should be natural choice to try before any more complex technique. In fact, it is not entirely obvious how a training-based approach should be compared to a post-hoc method. For instance, Feng et al. (2023) has found that, for some state-of-the-art training-based approaches to selective classification, *after* the main classifier has been trained with the corresponding technique, better selective classification performance can be obtained by discarding the auxiliary output providing confidence values and simply use the conventional MSP as the confidence estimator. Thus, in this sense, the MSP can be seen as a strong baseline.

Post-hoc methods have been widely considered in the context of calibration, among which the most popular approach is temperature scaling (TS). Applying TS to improve calibration (of the MSP confidence estimator) was originally proposed in (Guo et al., 2017) based on the negative log-likelihood. Optimizing TS for other metrics has been explored in (Mukhoti et al., 2020; Karandikar et al., 2021; Clarté et al., 2023) for calibration and in (Liang et al., 2023) for OOD detection, but had not been proposed for selective classification. A generalization of TS is adaptive TS (ATS) (Balanya et al., 2023), which uses an input-dependent temperature based on logits. The post-hoc methods we consider here can be seen as a special case of ATS, as logit norms may be seen as an input-dependent temperature; however Balanya et al. (2023) investigate a different temperature function and focuses on calibration. Other logit-based confidence estimators proposed for calibration and OOD detection include (Liu et al., 2020; Tomani et al., 2022; Rahimi et al., 2022; Neumann et al., 2018; Gonsior et al., 2022).

Normalizing the logits with the L_2 norm before applying the softmax function was used in (Kornblith et al., 2021) and later proposed and studied in (Wei et al., 2022) as a training technique (combined with TS) to improve OOD detection and calibration. A variation where the logits are normalized to unit variance was proposed in (Jiang et al., 2023) to accelerate training.

Benchmarking of models in their performance at selective classification/misclassification detection has been done in (Galil et al., 2023; Ding et al., 2020), however these works mostly consider the MSP as the confidence estimator. In the context of calibration, Wang et al. (2021) and Ashukha et al. (2020) have argued that models should be compared after simple post-hoc optimizations, since models that appear worse than others can sometimes easily be improved by methods such as TS. Here we advocate and provide further evidence for this approach in the context of selective classification.

B On the DOCTOR method

The paper by (Granese et al., 2021) introduces a selection mechanism named DOCTOR, which actually refers to two distinct methods, D_α and D_β , in two possible scenarios, Total Black Box and Partial Black Box. Only the former scenario corresponds to post-hoc estimators and, in this case, the two methods are equivalent to NegativeGini and MSP, respectively.

To see this, first consider the definition of D_α : a sample x is rejected if $1 - \hat{g}(x) > \gamma \hat{g}(x)$, where

$$1 - \hat{g}(x) = \sum_{k \in \mathcal{Y}} (\sigma(\mathbf{z}))_k (1 - (\sigma(\mathbf{z}))_k) = 1 - \sum_{k \in \mathcal{Y}} (\sigma(\mathbf{z}))_k^2 = 1 - \|\sigma(\mathbf{z})\|_2^2$$

is exactly the Gini index of diversity applied to the softmax outputs. Thus, a sample x is accepted if $1 - \hat{g}(x) \leq \gamma \hat{g}(x) \iff (1 + \gamma) \hat{g}(x) \geq 1 \iff \hat{g}(x) \geq 1/(1 + \gamma) \iff \hat{g}(x) - 1 \geq 1/(1 + \gamma) - 1$. Therefore, the method is equivalent to the confidence estimator $g(x) = \hat{g}(x) - 1 = \|\sigma(\mathbf{z})\|^2 - 1$, with $t = 1/(1 + \gamma) - 1$ as the selection threshold.

Now, consider the definition of D_β : a sample x is rejected if $\hat{P}_e(x) > \gamma(1 - \hat{P}_e(x))$, where $\hat{P}_e(x) = 1 - (\sigma(\mathbf{z}))_{\hat{y}}$ and $\hat{y} = \arg \max_{k \in \mathcal{Y}} (\sigma(\mathbf{z}))_k$, i.e., $\hat{P}_e(x) = 1 - \text{MSP}(\mathbf{z})$. Thus, a sample x is accepted if $\hat{P}_e(x) \leq \gamma(1 - \hat{P}_e(x)) \iff (1 + \gamma) \hat{P}_e(x) \leq \gamma \iff \hat{P}_e(x) \leq \gamma/(1 + \gamma) \iff \text{MSP}(\mathbf{z}) \geq 1 - \gamma/(1 + \gamma) = 1/(1 + \gamma)$. Therefore, the method is equivalent to the confidence estimator $g(x) = \text{MSP}(\mathbf{z})$, with $t = 1/(1 + \gamma)$ as the selection threshold.

Given the above results, one may wonder why the results in (Granese et al., 2021) show different performance values for D_β and MSP (softmax response), as shown, for instance, in Table 1 in Granese et al. (2021). We suspect this discrepancy is due to numerical imprecision in the computation of the ROC curve for a limited number of threshold values, as the authors themselves point out on their Appendix C.3, combined with the fact that D_β and MSP in (Granese et al., 2021) use different parametrizations for the threshold values. In contrast, we use the implementation from the scikit-learn library (adapting it as necessary for the RC curve), which considers every possible threshold for the confidence values given and so is immune to this kind of imprecision.

C More details and results on the experiments on ImageNet

C.1 Hyperparameter optimization of post-hoc methods

For not being differentiable, the NAURC metric demands a zero-order optimization. For this work, the optimizations of p and T were conducted via grid-search. Note that, as p approaches infinity, $\|\mathbf{z}\|_p \rightarrow \max(|\mathbf{z}|)$. Indeed, it tends to converge reasonable quickly. Thus, the grid search on p can be made only for small p . In our experiments, we noticed that it suffices to evaluate a few values of p , such as the integers between 0 and 10, where the 0-norm is taken here to mean the sum of all nonzero values of the vector. The temperature values were taken from the range between 0.01 and 3, with a step size of 0.01, as this showed to be sufficient for achieving the optimal temperature for selective classification (in general between 0 and 1).

C.2 AUROC results

Table 5 shows the AUROC results for all methods for an EfficientNetV2-XL on ImageNet, while Table 6 shows the same but for a VGG-16. As it can be seen, the results are consistent with the ones for NAURC presented in Section 4.

Table 5: AUROC[x100] for post-hoc methods for an EfficientNet-V2-XL for ImageNet

Confidence Estimation	Logit Transformation			
	Raw	TS-NLL	TS-AUROC	pNorm
MSP	0.7732	0.8109	0.8587	0.8708
SoftmaxMargin	0.7990	0.8246	0.8590	0.8718
MaxLogit	0.6347	0.6347	0.6347	0.8741
LogitsMargin	0.8604	0.8604	0.8604	0.8701
NegativeEntropy	0.6890	0.7710	0.7538	0.8238
NegativeGini	0.7669	0.8101	0.8588	0.8711

Table 6: AUROC[x100] for post-hoc methods for VGG16 for ImageNet

Confidence Estimation	Logit Transformation			
	Raw	TS-NLL	TS-AUROC	pNorm
MSP	0.8661	0.8652	0.8662	0.8662
SoftmaxMargin	0.8603	0.8610	0.8617	0.8617
MaxLogit	0.7884	0.7884	0.7884	0.8557
LogitsMargin	0.8478	0.8478	0.8478	0.8478
NegativeEntropy	0.8556	0.8492	0.8659	0.8659
NegativeGini	0.8645	0.8619	0.8661	0.8661

C.3 RC curves

In Figure 4 the RC curves of selected post-hoc methods applied to a few representative models are shown.

C.4 Effect of ϵ

Figure 5 shows the results (in APG metric) for all methods when p is optimized. As can be seen, MaxLogit-pNorm is dominant for all $\epsilon > 0$, indicating that, provided the MSP fallback described in Section 3.2.2 is enabled, it outperforms the other methods.

D Experiments on additional datasets

D.1 Experiments on Oxford-IIIT Pet

The hold-out set for Oxford-IIIT Pet, consisting of 500 samples, was taken from the training set before training. The model used was an EfficientNet-V2-XL pretrained on ImageNet from Wightman (2019). It was fine-tuned on Oxford-IIIT Pet (Parkhi et al., 2012). The training was conducted for 100 epochs with Cross Entropy Loss, using a SGD optimizer with initial learning rate of 0.1 and a Cosine Annealing learning rate schedule with period 100. Moreover, a weight decay of 0.0005 and a Nesterov’s momentum of 0.9 were used. Data transformations were applied, specifically standardization, random crop (for size 224x224) and random horizontal flip.

Figure 6 shows the RC curves for some selected methods for the EfficientNet-V2-XL. As can be seen, considerable gains are obtained with the optimization of p , especially in the low-risk region.

D.2 Experiments on CIFAR-100

The hold-out set for CIFAR-100, consisting of 5000 samples, was taken from the training set before training. The model used was forked from github.com/kuangliu/pytorch-cifar, and adapted for CIFAR-100 (Krizhevsky, 2009). It was trained for 200 epochs with Cross Entropy Loss, using a SGD optimizer with initial learning rate of 0.1 and a Cosine Annealing learning rate schedule with period 200. Moreover, a weight decay of 0.0005 and a Nesterov’s momentum of 0.9 were used. Data transformations were applied, specifically standardization, random crop (for size 32x32 with padding 4) and random horizontal flip.

Figure 7 shows the RC curves for some selected methods for a VGG19. As it can be seen, the results follow the same pattern of the ones observed for ImageNet, with MaxLogit-pNorm achieving the best results.

E Data Efficiency

As mentioned in Section 4, the experiments conducted in ImageNet used a hold-out dataset of 5,000 images randomly sampled from the validation dataset, resulting in 45,000 images reserved for the test phase.

In this section, the primary aim is to investigate the data efficiency of the methods, which indicates their capacity to learn and generalize from limited data. To accomplish this, the optimization process was executed multiple times, utilizing different fractions of the hold-out set while keeping the test set fixed at 45,000 samples. Consequently, two distinct types of random splits were implemented using the validation dataset. The first involved dividing the validation set into hold-out and test sets, while the second involved sampling fractions from the hold-out set. To ensure the findings were generalizable and robust, both of these random split procedures were repeated five times each, culminating in a total of 25 experiments for each analyzed fraction of the hold-out set.

Figure 8 displays the outcomes of these studies for an ResNet50 trained on ImageNet. As observed, MaxLogit-pNorm exhibits outstanding data efficiency, while methods that use temperature achieve lower efficiency.

Additionally, the data efficiency experiment was conducted on the VGG19 model for CIFAR-100. Indeed, the same conclusions hold about the high efficiency of MaxLogit-pNorm.

F When is post-hoc optimization beneficial?

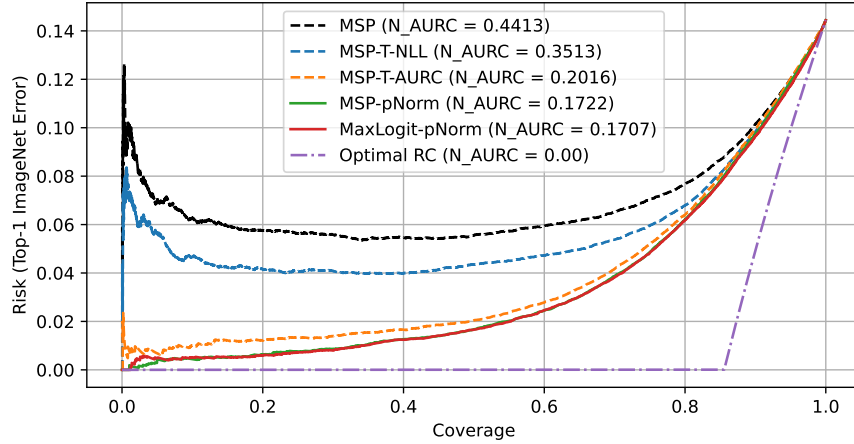
In this section we investigate in which circumstances post-hoc optimization yields significant gains. Figure 10 shows histograms of confidence values for two representative examples of non-improvable and improvable models, with the latter one shown before and after post-hoc optimization. Figure 11 shows the NAURC gain over MSP versus the proportion of samples with high MSP for each classifier. As can be seen, highly confident models tend to have a good MSP confidence estimator, while less confident models tend to have a poor confidence estimator that is easily improvable by post-hoc methods—after which the resulting confidence estimator becomes concentrated on high values.

G Selective classification under distribution shift

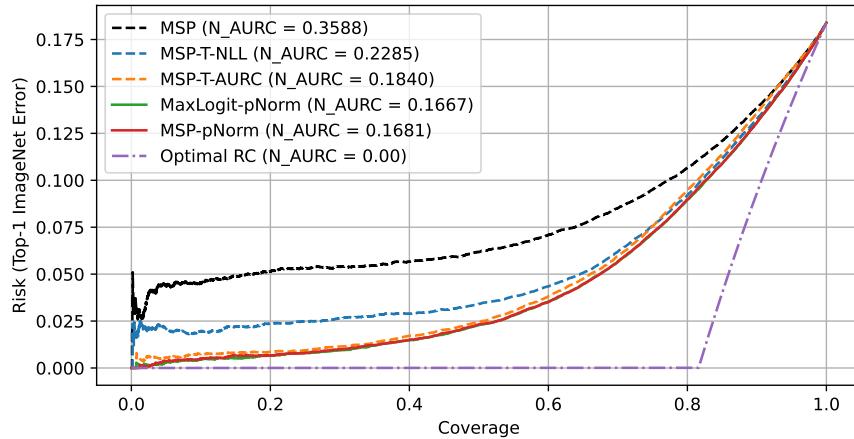
Figure 12a shows a plot of NAURC on ImageNetV2 versus NAURC on the ImageNet test set for all models evaluated. As can be seen, the results follow an affine function, especially after post-hoc optimization, indicating that the selective classification performance is consistent under distribution shift and can be estimated by the performance in the original distribution. Figure 12b shows NAURC versus accuracy on the ImageNetV2 dataset. As can be seen, post-hoc optimization, made in the original hold-out set, helps improve selective classification performance under distribution shift.

H Full Results on ImageNet

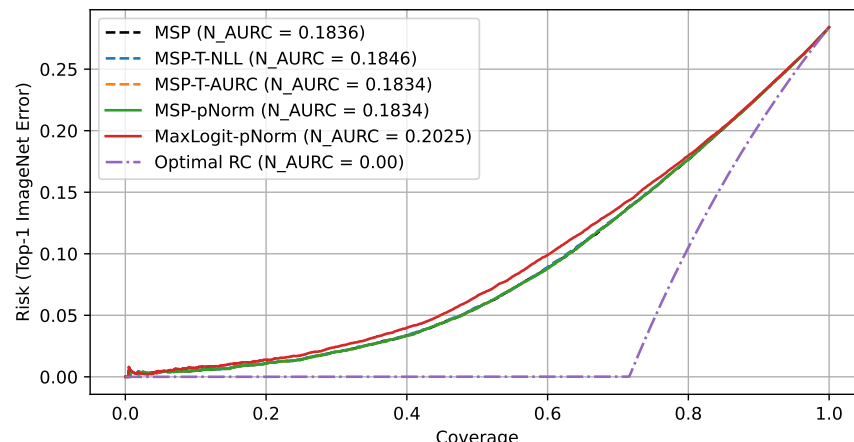
Table 7 presents all the NAURC results for the most relevant methods for all the evaluated models on ImageNet, while Table 8 shows the corresponding AURC results and Table 9 the corresponding AUROC results.



(a) EfficientNetV2-XL



(b) WideResNet50-2



(c) VGG16

Figure 4: RC curves for selected post-hoc methods applied to ImageNet classifiers.

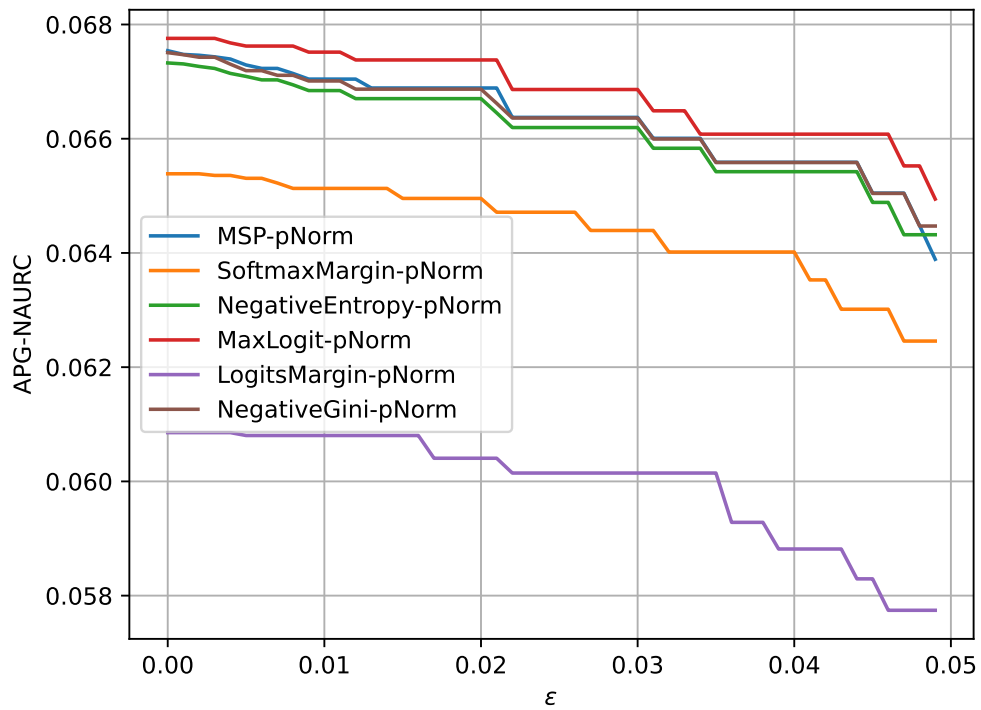


Figure 5: APG in terms of ϵ

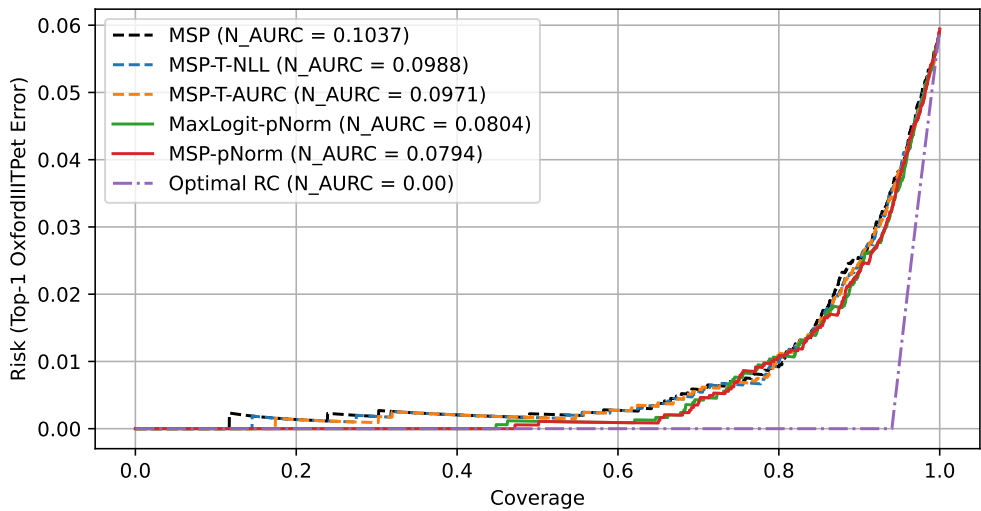


Figure 6: RC curves for a EfficientNet-V2-XL for Oxford-IIIT Pet

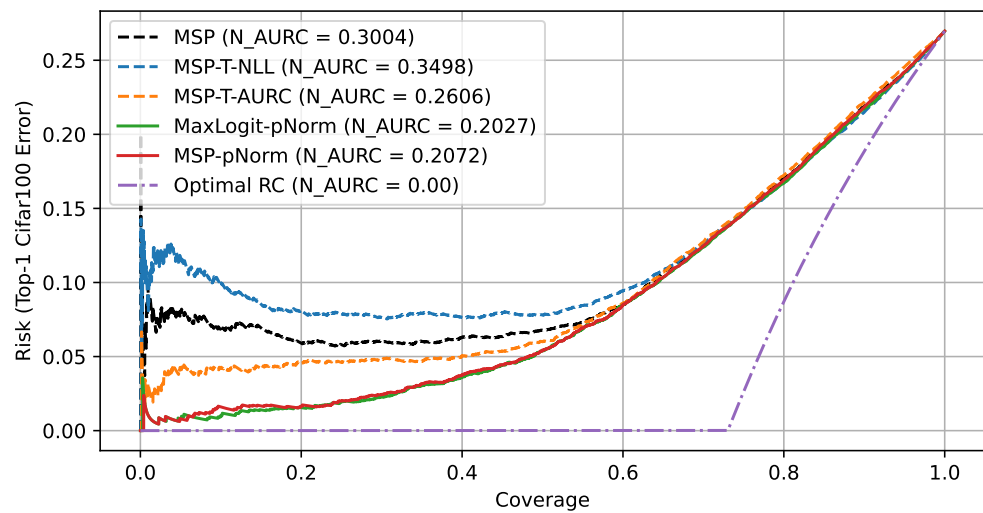


Figure 7: RC curves for a VGG19 for CIFAR-100

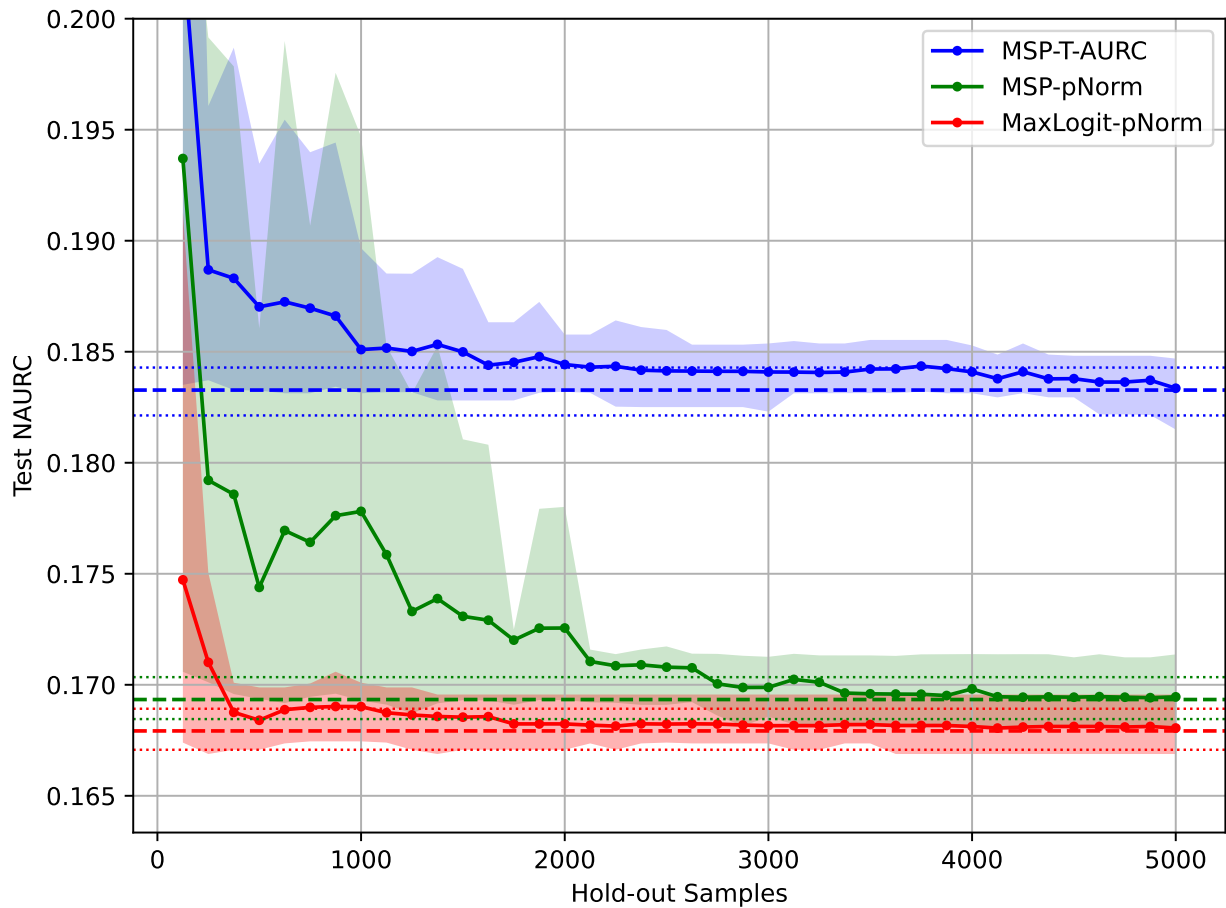


Figure 8: Data Efficiency: Average NAURC variation with number of hold-out samples used, for a ResNet50 on ImageNet. Dashed lines represent the optimal NAURC for each method, i.e., the achieved value when the optimization is made directly on the test set. Filled regions for each curve correspond to percentiles 10 and 90, while dotted lines represent the same but for the optimal value (optimized on test set directly).

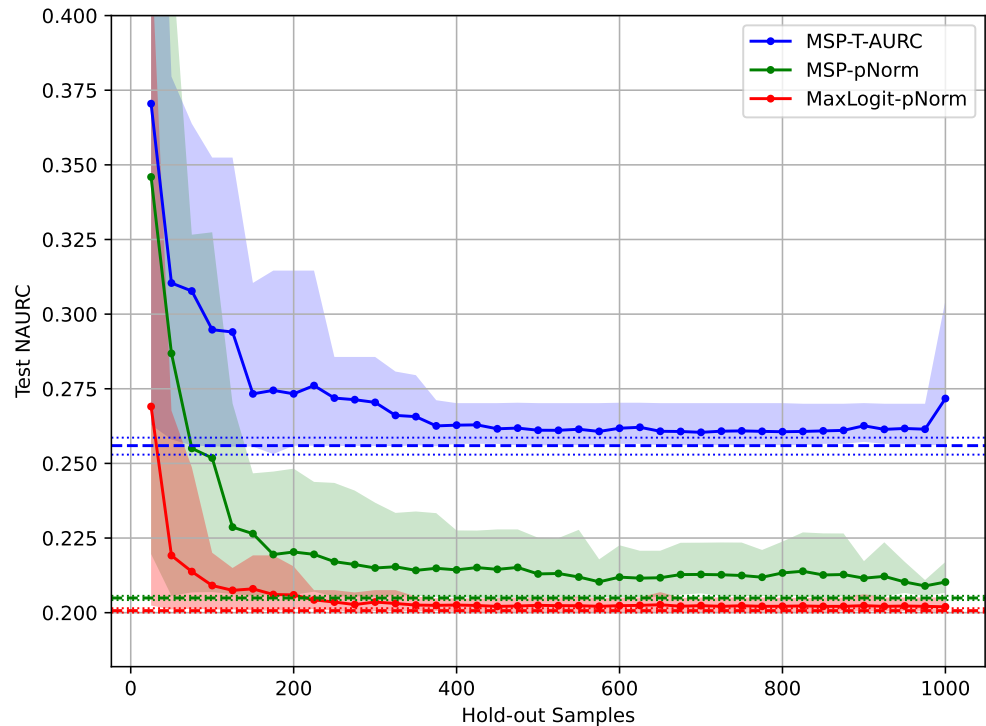
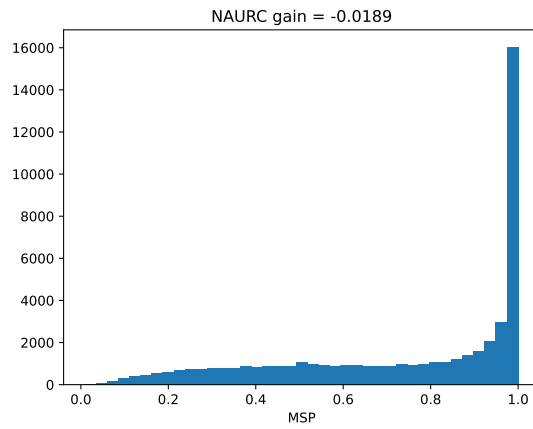
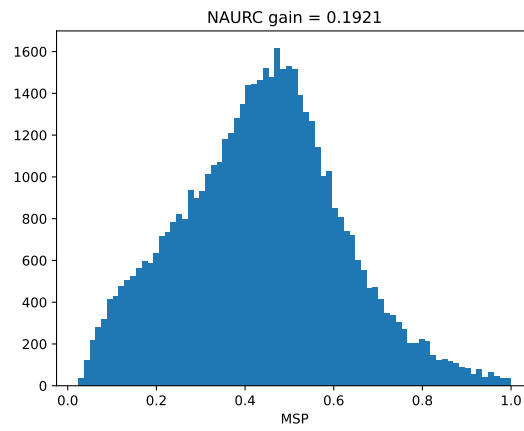


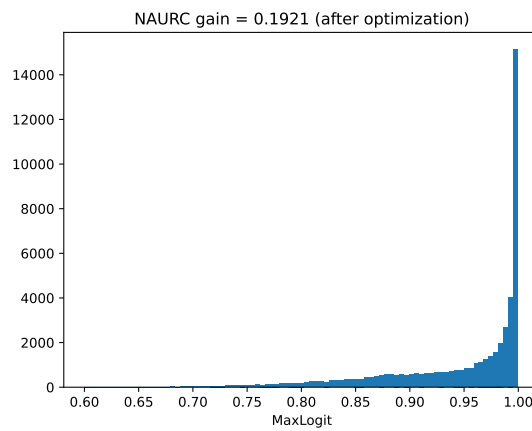
Figure 9: Data Efficiency: Average NAURC variation with number of hold-out samples used, for a VGG19 for CIFAR100. Dashed lines represent the optimal NAURC for each method, i.e., the achieved value when the optimization is made directly on the test set. Filled regions for each curve correspond to percentiles 10 and 90, while dotted lines represent the same but for the optimal value (optimized on test set directly).



(a) VGG16



(b) WideResNet50-2



(c) WideResNet50-2 after MaxLogit-pNorm optimization

Figure 10: Histograms of confidence values for VGG16 MSP, WideResNet50-2 MSP and WideResNet50-2 MaxLogit-pNorm on ImageNet.

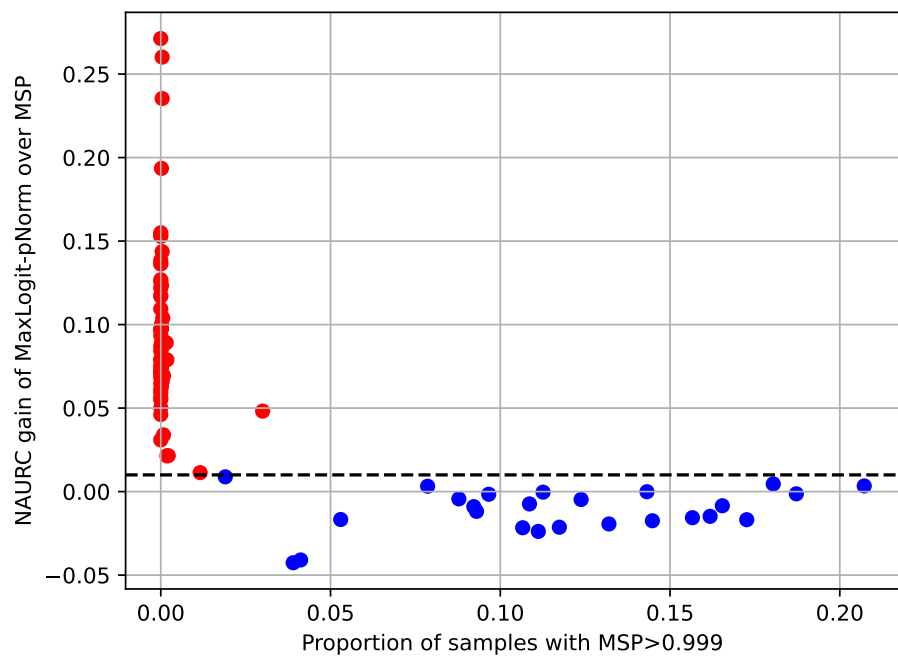
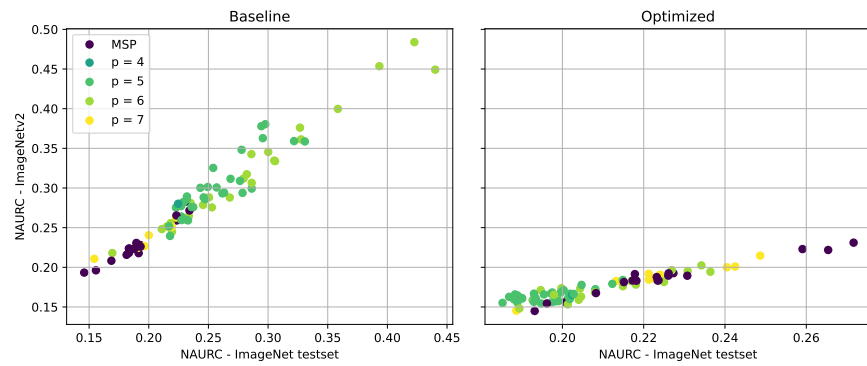
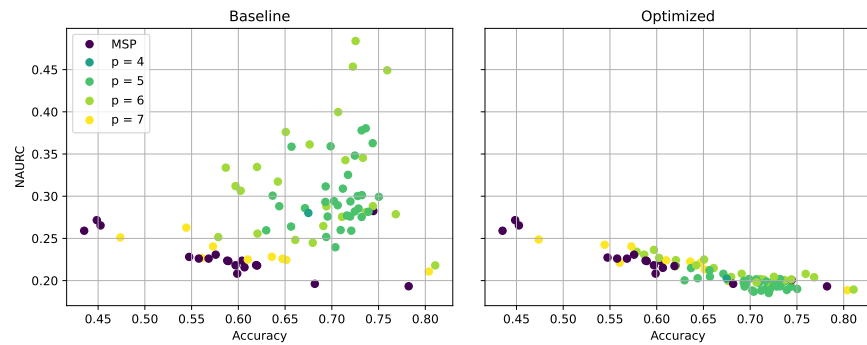


Figure 11: NAURC gain versus the proportion of samples with MSP > 0.999.



(a) NAURC on ImageNetV2 versus NAURC on the ImageNet test set



(b) NAURC versus accuracy on ImageNetV2

Figure 12: NAURC under distribution shift (ImageNetV2) for all models considered for ImageNet

Table 7: NAURC for all models evaluated on ImageNet

Model	Accuracy[%]	Method				
		MSP	MSP-TS-NLL	MSP-TS-AURC	LogitsMargin	MSP-pNorm - p^*
alexnet	0.5657	0.2234	0.2248	0.2232	0.2604	0.2232 - 0
convnext_base	0.8402	0.2977	0.2293	0.1795	0.1784	0.1613 - 4
convnext_large	0.8438	0.2956	0.2413	0.1772	0.1728	0.1582 - 5
convnext_small	0.8360	0.2944	0.2249	0.1733	0.1732	0.1580 - 3
convnext_tiny	0.8249	0.2860	0.2190	0.1832	0.1810	0.1605 - 5
densenet121	0.7439	0.1915	0.1926	0.1915	0.2095	0.1914 - 0
densenet161	0.7715	0.1904	0.1943	0.1903	0.2036	0.1831 - 3
densenet169	0.7555	0.1895	0.1923	0.1894	0.2046	0.1862 - 1
densenet201	0.7683	0.1894	0.1911	0.1887	0.2024	0.1844 - 3
efficientnet_b0	0.7768	0.2110	0.1962	0.1965	0.2004	0.1761 - 4
efficientnet_b1	0.7977	0.2194	0.1884	0.1819	0.1891	0.1745 - 4
efficientnet_b2	0.8054	0.2336	0.2062	0.1868	0.1929	0.1714 - 5
efficientnet_b3	0.8193	0.2529	0.2066	0.1810	0.1794	0.1651 - 5
efficientnet_b4	0.8333	0.3001	0.2147	0.1750	0.1763	0.1692 - 3
efficientnet_b5	0.8334	0.2350	0.1977	0.1704	0.1736	0.1574 - 4
efficientnet_b6	0.8389	0.2304	0.1930	0.1735	0.1705	0.1735 - 0
efficientnet_b7	0.8406	0.2505	0.2031	0.1639	0.1664	0.1550 - 3
efficientnet_v2_l	0.8574	0.2456	0.2061	0.1730	0.1734	0.1597 - 5
efficientnet_v2_m	0.8504	0.2863	0.2220	0.1768	0.1757	0.1646 - 3
efficientnet_v2_s	0.8413	0.2284	0.1918	0.1667	0.1698	0.1563 - 4
googlenet	0.6970	0.2154	0.2068	0.2052	0.2279	0.2024 - 3
inception_v3	0.7722	0.2273	0.2158	0.1973	0.2026	0.1800 - 4
maxvit_t	0.8362	0.2228	0.2024	0.1737	0.1735	0.1614 - 5
mnasnet0_5	0.6769	0.2229	0.2104	0.2086	0.2324	0.2014 - 3
mnasnet0_75	0.7110	0.3059	0.2124	0.2081	0.2252	0.1955 - 3
mnasnet1_0	0.7349	0.1833	0.1854	0.1834	0.2010	0.1833 - 0
mnasnet1_3	0.7640	0.3268	0.2093	0.1960	0.2039	0.1814 - 4
mobilenet_v2	0.7211	0.2795	0.2049	0.2020	0.2204	0.1943 - 4
mobilenet_v3_large	0.7529	0.2183	0.1953	0.1926	0.2099	0.1874 - 5
mobilenet_v3_small	0.6770	0.1929	0.1946	0.1926	0.2170	0.1926 - 0
regnet_x_16gf	0.8266	0.2271	0.2008	0.1743	0.1745	0.1619 - 4
regnet_x_1_6gf	0.7962	0.3277	0.2104	0.1899	0.1948	0.1740 - 4
regnet_x_32gf	0.8294	0.2373	0.2127	0.1719	0.1746	0.1621 - 3

regnet_x_3_2gf	0.8111	0.2679	0.2161	0.1928	0.1713 - 5
regnet_x_400mf	0.7483	0.3052	0.2072	0.1989	0.2111
regnet_x_800mf	0.7748	0.3308	0.2128	0.1986	0.2067
regnet_x_8gf	0.8166	0.2320	0.2013	0.1754	0.1778
regnet_y_128gf	0.8819	0.1543	0.1553	0.1489	0.1525
regnet_y_16gf	0.8284	0.2786	0.2271	0.1726	0.1700
regnet_y_1_6gf	0.8085	0.2617	0.2113	0.1893	0.1910
regnet_y_32gf	0.8332	0.2432	0.2038	0.1693	0.1701
regnet_y_3_2gf	0.8189	0.2318	0.1980	0.1811	0.1841
regnet_y_400mf	0.7578	0.2569	0.2144	0.2047	0.2164
regnet_y_800mf	0.7881	0.2474	0.2036	0.1909	0.1999
regnet_y_8gf	0.8273	0.2291	0.1928	0.1703	0.1711
resnet101	0.8185	0.2632	0.2176	0.1825	0.1832
resnet152	0.8225	0.2540	0.2081	0.1702	0.1716
resnet18	0.6971	0.2000	0.2018	0.1994	0.2208
resnet34	0.7326	0.1913	0.1928	0.1914	0.2107
resnet50	0.8082	0.3218	0.2109	0.1814	0.1841
resnext101_32x8d	0.8276	0.4226	0.2542	0.1863	0.1836
resnext101_64x4d	0.8316	0.3933	0.2332	0.1763	0.1746
resnext50_32x4d	0.8116	0.2685	0.2206	0.1843	0.1870
shufflenet_v2_x0.5	0.6052	0.2192	0.2218	0.2180	0.2412
shufflenet_v2_x1.0	0.6924	0.1965	0.2005	0.1961	0.2107
shufflenet_v2_x1.5	0.7299	0.2863	0.2122	0.2072	0.2233
shufflenet_v2_x2_0	0.7616	0.2822	0.2041	0.1938	0.2024
squeezeNet1_0	0.5804	0.2341	0.2363	0.2318	0.2618
squeezeNet1_1	0.5817	0.2232	0.2249	0.2220	0.2546
swin_b	0.8353	0.2778	0.2420	0.1764	0.1773
swin_s	0.8316	0.2329	0.2145	0.1813	0.1808
swin_t	0.8143	0.2170	0.1956	0.1801	0.1850
vgg11	0.6909	0.1931	0.1941	0.1757	0.1780
vgg11_bn	0.7034	0.1896	0.1909	0.1895	0.2114
vgg13	0.6988	0.1898	0.1907	0.1895	0.2108
vgg13_bn	0.7151	0.1880	0.1895	0.1878	0.2098
vgg16	0.7156	0.1838	0.1850	0.1836	0.2047
vgg16_bn	0.7335	0.1814	0.1833	0.1813	0.1993
vgg19	0.7232	0.1832	0.1841	0.1831	0.2044

vgg19_bn	0.7420	0.1834	0.1851	0.1834	0.2008	0.1834 - 0
vit_b_16	0.8102	0.2359	0.2113	0.1815	0.1831	0.1669 - 4
vit_b_32	0.7592	0.2274	0.2092	0.1903	0.1944	0.1719 - 4
vit_h_14	0.8848	0.1695	0.1652	0.1533	0.1557	0.1483 - 4
vit_l_16	0.7969	0.2246	0.2146	0.1841	0.1869	0.1652 - 4
vit_l_32	0.7696	0.2460	0.2290	0.1932	0.1930	0.1664 - 4
wide_resnet101_2	0.8246	0.2765	0.2255	0.1799	0.1769	0.1606 - 5
wide_resnet50_2	0.8155	0.3585	0.2284	0.1830	0.1852	0.1663 - 4
efficientnetv2_xl	0.8555	0.4401	0.3504	0.2056	0.1935	0.1714 - 4
vit_l_16_384	0.8702	0.1459	0.1461	0.1451	0.1526	0.1450 - 0
vit_b_16_sam	0.8016	0.1557	0.1555	0.1546	0.1614	0.1545 - 0
vit_b_32_sam	0.7368	0.1687	0.1682	0.1676	0.1789	0.1676 - 0

Table 8: AURC for all models evaluated on ImageNet

Model	Accuracy[%]						Method			
	MSP	MSP-TS-NLL	MSP-TS-AURC	LogitsMargin	MSP-pNorm - p^*	MaxLogit-pNorm - p^*				
alexnet	0.5657	0.1840	0.1845	0.1840	0.1959	0.1839 - 0				0.1894 - 0
convnext_base	0.8402	0.0570	0.0470	0.0398	0.0396	0.0371 - 4				0.0370 - 5
convnext_large	0.8438	0.0553	0.0475	0.0383	0.0377	0.0355 - 5				0.0354 - 5
convnext_small	0.8360	0.0583	0.0479	0.0402	0.0402	0.0379 - 3				0.0376 - 5
convnext_tiny	0.8249	0.0617	0.0511	0.0454	0.0450	0.0417 - 5				0.0415 - 6
densenet121	0.7439	0.0782	0.0784	0.0781	0.0821	0.0781 - 0				0.0797 - 0
densenet161	0.7715	0.0665	0.0672	0.0665	0.0691	0.0650 - 3				0.0658 - 7
densenet169	0.7555	0.0728	0.0734	0.0728	0.0760	0.0721 - 1				0.0730 - 7
densenet201	0.7683	0.0675	0.0679	0.0674	0.0702	0.0665 - 3				0.0675 - 7
efficientnet_b0	0.7768	0.0684	0.0655	0.0656	0.0663	0.0615 - 4				0.0616 - 6
efficientnet_b1	0.7977	0.0616	0.0560	0.0548	0.0561	0.0534 - 4				0.0532 - 6
efficientnet_b2	0.8054	0.0610	0.0562	0.0529	0.0539	0.0501 - 5				0.0500 - 6
efficientnet_b3	0.8193	0.0587	0.0512	0.0470	0.0467	0.0443 - 5				0.0441 - 6
efficientnet_b4	0.8333	0.0604	0.0474	0.0413	0.0415	0.0404 - 3				0.0399 - 7
efficientnet_b5	0.8334	0.0504	0.0447	0.0406	0.0411	0.0386 - 4				0.0384 - 6
efficientnet_b6	0.8389	0.0477	0.0422	0.0393	0.0389	0.0393 - 0				0.0367 - 0
efficientnet_b7	0.8406	0.0500	0.0431	0.0374	0.0377	0.0360 - 3				0.0358 - 6
efficientnet_v2_l	0.8574	0.0431	0.0379	0.0335	0.0336	0.0317 - 5				0.0316 - 6
efficientnet_v2_m	0.8504	0.0513	0.0424	0.0362	0.0360	0.0345 - 3				0.0339 - 5
efficientnet_v2_s	0.8413	0.0465	0.0412	0.0376	0.0380	0.0360 - 4				0.0359 - 5
googlenet	0.6970	0.1056	0.1034	0.1030	0.1088	0.1023 - 3				0.1027 - 6
inception_v3	0.7722	0.0736	0.0713	0.0676	0.0686	0.0641 - 4				0.0639 - 5
maxvit_t	0.8362	0.0476	0.0445	0.0402	0.0402	0.0383 - 5				0.0381 - 5
mnasnet0_5	0.6769	0.1178	0.1146	0.1141	0.1204	0.1121 - 3				0.1121 - 7
mnasnet0_75	0.7110	0.1207	0.0980	0.0970	0.1011	0.0939 - 3				0.0941 - 6
mnasnet1_0	0.7349	0.0802	0.0807	0.0803	0.0843	0.0802 - 0				0.0821 - 0
mnasnet1_3	0.7640	0.0975	0.0734	0.0706	0.0723	0.0676 - 4				0.0676 - 6
mobilenet_v2	0.7211	0.1090	0.0914	0.0908	0.0951	0.0889 - 4				0.0891 - 6
mobilenet_v3_large	0.7529	0.0801	0.0752	0.0746	0.0783	0.0734 - 5				0.0734 - 6
mobilenet_v3_small	0.6770	0.1099	0.1103	0.1098	0.1162	0.1097 - 0				0.1129 - 0
regnet_x_16gf	0.8266	0.0517	0.0476	0.0434	0.0435	0.0414 - 4				0.0413 - 5
regnet_x_1_6gf	0.7962	0.0818	0.0605	0.0568	0.0577	0.0539 - 4				0.0538 - 6
regnet_x_32gf	0.8294	0.0523	0.0485	0.0421	0.0425	0.0406 - 3				0.0400 - 5

regnet_x_3_2gf	0.8111	0.0646	0.0558	0.0518	0.0481 - 5
regnet_x_400mf	0.7483	0.1009	0.0797	0.0779	0.0743 - 4
regnet_x_800mf	0.7748	0.0929	0.0696	0.0668	0.0626 - 4
regnet_x_8gf	0.8166	0.0563	0.0513	0.0470	0.0452 - 3
regnet_y_128gf	0.8819	0.0244	0.0245	0.0238	0.0234 - 4
regnet_y_16gf	0.8284	0.0591	0.0511	0.0426	0.0422
regnet_y_1_6gf	0.8085	0.0646	0.0559	0.0522	0.0485 - 4
regnet_y_32gf	0.8332	0.0517	0.0458	0.0405	0.0384 - 3
regnet_y_3_2gf	0.8189	0.0554	0.0499	0.0471	0.0448 - 5
regnet_y_400mf	0.7578	0.0861	0.0771	0.0751	0.0707 - 4
regnet_y_800mf	0.7881	0.0707	0.0624	0.0601	0.0566 - 4
regnet_y_8gf	0.8273	0.0518	0.0461	0.0426	0.0405 - 5
resnet101	0.8185	0.0607	0.0533	0.0475	0.0476
resnet152	0.8225	0.0576	0.0502	0.0441	0.0444
resnet18	0.6971	0.1017	0.1021	0.1015	0.1016 - 1
resnet34	0.7326	0.0830	0.0834	0.0831	0.0875
resnet50	0.8082	0.0751	0.0560	0.0509	0.0514
resnext101_32x8d	0.8276	0.0820	0.0556	0.0450	0.0446
resnext101_64x4d	0.8316	0.0754	0.0508	0.0421	0.0418
resnext50_32x4d	0.8116	0.0645	0.0563	0.0502	0.0507
shufflenet_v2_x0.5	0.6052	0.1575	0.1583	0.1571	0.1642
shufflenet_v2_x1.0	0.6924	0.1031	0.1041	0.1030	0.1067
shufflenet_v2_x1.5	0.7299	0.1061	0.0890	0.0879	0.0916
shufflenet_v2_x2_0	0.7616	0.0895	0.0733	0.0712	0.0730
squeezeNet1_0	0.5804	0.1777	0.1784	0.1770	0.1865
squeezeNet1_1	0.5817	0.1735	0.1740	0.1731	0.1834
swin_b	0.8353	0.0561	0.0508	0.0409	0.0410
swin_s	0.8316	0.0507	0.0479	0.0428	0.0428
swin_t	0.8143	0.0547	0.0511	0.0486	0.0494
swin_v2_b	0.8412	0.0496	0.0456	0.0389	0.0392
swin_v2_s	0.8365	0.0488	0.0447	0.0394	0.0396
swin_v2_t	0.8204	0.0526	0.0485	0.0456	0.0462
vgg11	0.6909	0.1030	0.1032	0.1029	0.1089
vgg11_bn	0.7034	0.0961	0.0964	0.0960	0.1015
vgg13	0.6988	0.0983	0.0985	0.0982	0.1036
vgg13_bn	0.7151	0.0902	0.0905	0.0901	0.0954
vgg16	0.7156	0.0890	0.0892	0.0889	0.0940
vgg16_bn	0.7335	0.0804	0.0808	0.0804	0.0845
vgg19	0.7232	0.0853	0.0856	0.0903	0.0853 - 0

vgg19_bn	0.7420	0.0772	0.0775	0.0810	0.0771 - 0	0.0808 - 0
vit_b_16	0.8102	0.0595	0.0553	0.0502	0.0505	0.0477 - 4
vit_b_32	0.7592	0.0792	0.0754	0.0714	0.0723	0.0675 - 4
vit_h_14	0.8848	0.0253	0.0248	0.0235	0.0238	0.0229 - 4
vit_l_16	0.7969	0.0628	0.0610	0.0555	0.0560	0.0520 - 4
vit_l_32	0.7696	0.0784	0.0750	0.0678	0.0678	0.0624 - 4
wide_resnet101_2	0.8246	0.0603	0.0522	0.0450	0.0445	0.0419 - 5
wide_resnet50_2	0.8155	0.0778	0.0562	0.0486	0.0490	0.0458 - 4
efficientnetv2_xl	0.8555	0.0698	0.0578	0.0384	0.0368	0.0338 - 4
vit_l16_384	0.8702	0.0265	0.0265	0.0264	0.0273	0.0263 - 0
vit_b_16_sam	0.8016	0.0487	0.0487	0.0485	0.0497	0.0485 - 0
vit_b_32_sam	0.7368	0.0761	0.0760	0.0759	0.0784	0.0758 - 0

Table 9: AUROC for all models evaluated on ImageNet

Model	Accuracy[%]						Method			
	MSP	MSP-TS-NLL	MSP-TS-AURC	LogitsMargin	MSP-pNorm - p^*	MaxLogit-pNorm - p^*				
alexnet	0.5657	0.8483	0.8475	0.8483	0.8181	0.8482 - 0	0.8391 - 0			
convnext_base	0.8402	0.8255	0.8537	0.8672	0.8652	0.8769 - 4	0.8771 - 5			
convnext_large	0.8438	0.8257	0.8496	0.8700	0.8686	0.8793 - 5	0.8796 - 5			
convnext_small	0.8360	0.8271	0.8560	0.8702	0.8678	0.8780 - 3	0.8801 - 5			
convnext_tiny	0.8249	0.8247	0.8560	0.8659	0.8633	0.8781 - 5	0.8786 - 6			
densenet121	0.7439	0.8604	0.8596	0.8604	0.8454	0.8603 - 0	0.8564 - 0			
densenet161	0.7715	0.8635	0.8612	0.8633	0.8520	0.8668 - 3	0.8643 - 7			
densenet169	0.7555	0.8654	0.8634	0.8654	0.8520	0.8663 - 1	0.8631 - 7			
densenet201	0.7683	0.8628	0.8616	0.8630	0.8512	0.8647 - 3	0.8619 - 7			
efficientnet_b0	0.7768	0.8570	0.8642	0.8581	0.8535	0.8704 - 4	0.8701 - 6			
efficientnet_b1	0.7977	0.8538	0.8672	0.8676	0.8584	0.8711 - 4	0.8713 - 6			
efficientnet_b2	0.8054	0.8509	0.8628	0.8632	0.8592	0.8740 - 5	0.8740 - 6			
efficientnet_b3	0.8193	0.8435	0.8636	0.8701	0.8660	0.8770 - 5	0.8775 - 6			
efficientnet_b4	0.8333	0.8213	0.8600	0.8697	0.8668	0.8739 - 3	0.8750 - 7			
efficientnet_b5	0.8334	0.8549	0.8691	0.8724	0.8693	0.8809 - 4	0.8817 - 6			
efficientnet_b6	0.8389	0.8575	0.8714	0.8750	0.8704	0.8750 - 0	0.8811 - 0			
efficientnet_b7	0.8406	0.8509	0.8676	0.8761	0.8730	0.8814 - 3	0.8827 - 6			
efficientnet_v2_l	0.8574	0.8467	0.8645	0.8724	0.8700	0.8796 - 5	0.8798 - 6			
efficientnet_v2_m	0.8504	0.8251	0.8549	0.8696	0.8680	0.8750 - 3	0.8779 - 5			
efficientnet_v2_s	0.8389	0.8575	0.8714	0.8740	0.8707	0.8810 - 4	0.8815 - 5			
googlenet	0.6970	0.8490	0.8542	0.8550	0.8361	0.8563 - 3	0.8552 - 6			
inception_v3	0.7722	0.8491	0.8548	0.8605	0.8537	0.8700 - 4	0.8702 - 5			
maxvit_t	0.8362	0.8594	0.8658	0.8698	0.8672	0.8776 - 5	0.8781 - 5			
mnasnet0_5	0.6769	0.8465	0.8534	0.8536	0.8333	0.8577 - 3	0.8574 - 7			
mnasnet0_75	0.7110	0.8025	0.8510	0.8526	0.8377	0.8592 - 3	0.8584 - 6			
mnasnet1_0	0.7349	0.8659	0.8643	0.8658	0.8506	0.8658 - 0	0.8601 - 0			
mnasnet1_3	0.7640	0.7942	0.8554	0.8592	0.8501	0.8665 - 4	0.8662 - 6			
mobilenet_v2	0.7211	0.8167	0.8554	0.8559	0.8399	0.8600 - 4	0.8593 - 6			
mobilenet_v3_large	0.7529	0.8519	0.8625	0.8620	0.8464	0.8638 - 5	0.8636 - 6			
mobilenet_v3_small	0.6770	0.8621	0.8611	0.8622	0.8415	0.8622 - 0	0.8547 - 0			
regnet_x_16gf	0.8266	0.8553	0.8664	0.8703	0.8675	0.8777 - 4	0.8781 - 5			
regnet_x_1_6gf	0.7962	0.7991	0.8584	0.8627	0.8575	0.8718 - 4	0.8720 - 6			
regnet_x_32gf	0.8294	0.8551	0.8643	0.8717	0.8685	0.8766 - 3	0.8794 - 5			

regnet_x_3_2gf	0.8111	0.8340	0.8583	0.8592	0.8722 - 5
regnet_x_400mf	0.7483	0.8133	0.8583	0.8457	0.8660 - 4
regnet_x_800mf	0.7748	0.7981	0.8562	0.8593	0.8691 - 4
regnet_x_8gf	0.8166	0.8532	0.8656	0.8698	0.8750 - 3
regnet_y_128gf	0.8819	0.8836	0.8832	0.8835	0.8857 - 4
regnet_y_16gf	0.8284	0.8397	0.8590	0.8715	0.8697
regnet_y_1_6gf	0.8085	0.8396	0.8616	0.8660	0.8588
regnet_y_32gf	0.8332	0.8488	0.8642	0.8714	0.8684
regnet_y_3_2gf	0.8189	0.8522	0.8654	0.8672	0.8615
regnet_y_400mf	0.7578	0.8386	0.8575	0.8574	0.8448
regnet_y_800mf	0.7881	0.8413	0.8610	0.8613	0.8521
regnet_y_8gf	0.8273	0.8526	0.8683	0.8718	0.8687
resnet101	0.8185	0.8423	0.8604	0.8665	0.8631
resnet152	0.8225	0.8465	0.8652	0.8722	0.8691
resnet18	0.6971	0.8573	0.8561	0.8577	0.8398
resnet34	0.7326	0.8619	0.8608	0.8618	0.8456
resnet50	0.8082	0.8060	0.8602	0.8658	0.8617
resnext101_32x8d	0.8276	0.7680	0.8447	0.8654	0.8635
resnext101_64x4d	0.8316	0.7796	0.8534	0.8701	0.8684
resnext50_32x4d	0.8116	0.8360	0.8569	0.8644	0.8606
shufflenet_v2_x0.5	0.6052	0.8513	0.8498	0.8519	0.8319
shufflenet_v2_x1.0	0.6924	0.8602	0.8578	0.8602	0.8469
shufflenet_v2_x1.5	0.7299	0.8123	0.8518	0.8536	0.8390
shufflenet_v2_x2_0	0.7616	0.8170	0.8588	0.8617	0.8524
squeezeNet1_0	0.5804	0.8424	0.8410	0.8437	0.8319
squeezeNet1_1	0.5817	0.8486	0.8476	0.8492	0.8227
swin_b	0.8353	0.8432	0.8548	0.8678	0.8653
swin_s	0.8316	0.8554	0.8615	0.8667	0.8631
swin_t	0.8143	0.8588	0.8668	0.8683	0.8612
swin_v2_b	0.8412	0.8516	0.8604	0.8672	0.8645
swin_v2_s	0.8365	0.8592	0.8680	0.8733	0.8703
swin_v2_t	0.8204	0.8593	0.8683	0.8696	0.8647
vgg11	0.6909	0.8609	0.8602	0.8612	0.8410
vgg11_bn	0.7034	0.8626	0.8617	0.8627	0.8444
vgg13	0.6988	0.8619	0.8613	0.8622	0.8442
vgg13_bn	0.7151	0.8634	0.8623	0.8635	0.8451
vgg16	0.7156	0.8661	0.8652	0.8662	0.8478
vgg16_bn	0.7335	0.8679	0.8665	0.8680	0.8525
vgg19	0.7232	0.8656	0.8647	0.8656	0.8479

vgg19_bn	0.7420	0.8654	0.8641	0.8510	0.8654 - 0
vit_b_16	0.8102	0.8559	0.8637	0.8621	0.8756 - 4
vit_b_32	0.7592	0.8559	0.8631	0.8623	0.8556
vit_h_14	0.8848	0.8754	0.8777	0.8816	0.8742 - 4
vit_l_16	0.7969	0.8587	0.8618	0.8642	0.8848 - 4
vit_l_32	0.7696	0.8542	0.8591	0.8631	0.8850 - 6
wide_resnet101_2	0.8246	0.8384	0.8592	0.8691	0.8790 - 0
wide_resnet50_2	0.8155	0.7920	0.8524	0.8646	0.8752 - 6
efficientnetv2_xl	0.8555	0.7732	0.8109	0.8587	0.8767 - 4
vit_l_16_384	0.8702	0.8857	0.8855	0.8862	0.8750 - 5
vit_b_16_sam	0.8016	0.8825	0.8827	0.8833	0.8832 - 0
vit_b_32_sam	0.7368	0.8754	0.8758	0.8762	0.8825 - 0
					0.8755 - 0